AD-A191 277 DEVELOPMENT OF COST-EFFECTIVE MANUFACTURING PROCESS FOR 1/1
PRODUCING CERAMIC.. (U) ALLIED-SIGNAL CORP TORRANCE CA
GARRETT AUTOMOTIVE GROUP R J KOBAYASHI ET AL.
UNCLASSIFIED 14 AUG 87 TACOM-TR-13270-VOL-1 F/G 11/2 NL

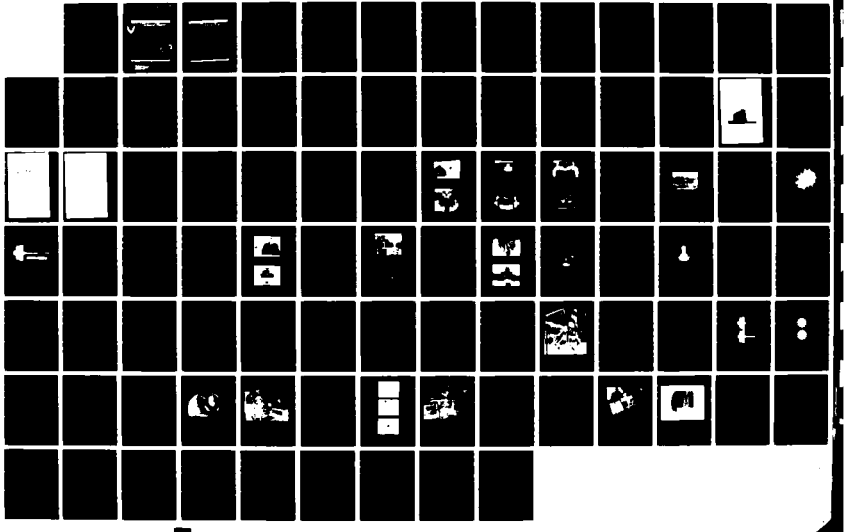

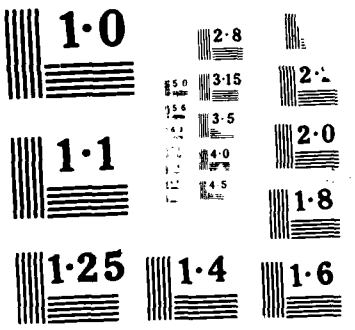
1·0
1·1
1·25
1·4
1·6
1·8
2·0
2·8
3·15
3·5
4·0
4·5

AD-A191 277

RD&E CENTER

Technical Report

No. 13270

DEVELOPMENT OF COST-EFFECTIVE MANUFACTURING PROCESS FOR PRODUCING CERAMIC TURBOCHARGER ROTORS

CONTRACT NUMBER DAAE 07-85-C-R 147

VOLUME 1 OF 2

AUGUST, 1987

By Robert J. Kobayashi, Robert L. Mullen
Donald E. Baker
Garrett Automotive Group,
Allied/Signal Corporation
3201 W. Lomita Blvd.
Torrance, CA 90501
and
Dr. Hun C. Yeh
AiResearch Casting Company
Allied/Signal Corporation
19800 Van Ness Ave.
Torrance, CA 90509

U.S. ARMY TANK-AUTOMOTIVE COMMAND
RESEARCH, DEVELOPMENT & ENGINEERING CENTER
Warren, Michigan 48397-5000

4

RD&E CENTER

Technical Report

No. 13270

DEVELOPMENT OF COST-EFFECTIVE
MANUFACTURING PROCESS FOR PRODUCING
CERAMIC TURBOCHARGER ROTORS

CONTRACT NUMBER DAAE 07-85-C-R 147

VOLUME 1 OF 2

AUGUST, 1987

Robert J. Kobayashi, Robert L. Mullen
Donald E. Baker
Garrett Automotive Group,
Allied/Signal Corporation
3201 W. Lomita Blvd.
Torrance, CA 90501

and

Dr. Hun C. Yeh
AiResearch Casting Company
Allied/Signal Corporation
19800 Van Ness Ave.
Torrance, CA 90509

By

U.S. ARMY TANK-AUTOMOTIVE COMMAND
RESEARCH, DEVELOPMENT & ENGINEERING CENTER
Warren, Michigan 48397-5000

NOTICES

This report is not to be construed as an official Department of the Army position.

Mention of any trade names or manufacturers in this report shall not be construed as an official endorsement or approval of such products or companies by the U.S. Government.

Destroy this report when it is no longer needed. Do not return it to the originator.

REPORT DOCUMENTATION PAGE

Form Approved
OMB No. 0704-0188
Exp. Date: Jun 30, 1986

1a. REPORT SECURITY CLASSIFICATION	1b. RESTRICTIVE MARKINGS
2a. SECURITY CLASSIFICATION AUTHORITY	3. DISTRIBUTION/AVAILABILITY OF REPORT: Approved for Public Release Distribution Unlimited
2b. DECLASSIFICATION/DOWNGRADING SCHEDULE	
4. PERFORMING ORGANIZATION REPORT NUMBER(S)	5. MONITORING ORGANIZATION REPORT NUMBER(S): 13271
6a. NAME OF PERFORMING ORGANIZATION: Garrett Automotive Group; 6b. OFFICE SYMBOL (If applicable):	7a. NAME OF MONITORING ORGANIZATION: U.S. Army Tank Automotive Command
6c. ADDRESS (City, State, and ZIP Code): 3201 W. Lomita Blvd. Torrance, CA 90505	7b. ADDRESS (City, State, and ZIP Code): AMSTA-TMC Warren, MI 48397-5000
8a. NAME OF FUNDING/SPONSORING ORGANIZATION; 8b. OFFICE SYMBOL (If applicable):	9. PROCUREMENT INSTRUMENT IDENTIFICATION NUMBER: DAAE07 - 85 - C - R147
8c. ADDRESS (City, State, and ZIP Code)	10. SOURCE OF FUNDING NUMBERS

PROGRAM ELEMENT NO.	PROJECT NO.	TASK NO.	WORK UNIT ACCESSION NO
78011	DE64	4856123	

11. TITLE (Include Security Classification)
Development of cost-effective manufacturing process for producing ceramic turbocharger rotors (u).

12. PERSONAL AUTHOR(S) Kobayashi, Robert J., Mullen, Robert L., and Baker, Donald E. (Garrett Automotive), and Yeh, Dr. Hun C. (AiResearch Casting Company)

13a. TYPE OF REPORT	13b. TIME COVERED	14. DATE OF REPORT (Year, Month, Day)	15. PAGE COUNT
Final	FROM 85 Oct TO 87 Jun	87 August 14	190

16. SUPPLEMENTARY NOTATION

17. COSATI CODES			18. SUBJECT TERMS (Continue on reverse if necessary and identify by block number)
FIELD	GROUP	SUB-GROUP	Ceramic rotor, turbocharger, shaftwheel assembly, silicon nitride, slip casting, ceramic rotor design, ceramic rotor fabrication, ceramic rotor turbocharger testing.

19. ABSTRACT (Continue on reverse if necessary and identify by block number)

Ceramic turbine rotors for turbochargers, because of the material's low density, offer faster turbocharger rotor acceleration which improves engine response and vehicle acceleration. Ceramics use relatively low cost materials in place of the currently used expensive, exotic and sometimes scarce metal elements and, hopefully, will allow the production of less expensive rotors. Only in the past few years have prototype ceramic rotors been produced. The U.S. Army Tank-Automotive Command (TACOM) established a program to demonstrate the feasibility of producing a cost effective ceramic rotor for military use with Garrett Automotive as the prime contractor and The AiResearch Casting Company (ACC) as the major sub-contractor. While ACC has been able to produce small (passenger car) ceramic rotors, within the timeframe of this program, ACC was not able to produce a satisfactory large turbocharger rotor. A major goal of this program was to develop a domestic source for rotor production, but from Garrett's experience no other U.S. company was capable. Therefore, to conclude the program with demonstration hardware, a Japanese supplier of known capability (Kyocera) was asked to make the rotors. Kyocera produced ceramic rotors were assembled into turbochargers (Model TV81) and successfully qualified through a series of performance and durability tests. Because of the complex processing, the current cost of a ceramic rotor is substantially more expensive than that of a metal rotor.

20. DISTRIBUTION/AVAILABILITY OF ABSTRACT	21. ABSTRACT SECURITY CLASSIFICATION
☒ UNCLASSIFIED/UNLIMITED ☐ SAME AS RPT. ☐ DTIC USERS	Unclassified

22a. NAME OF RESPONSIBLE INDIVIDUAL	22b. TELEPHONE (Include Area Code)	22c. OFFICE SYMBOL
Don Ostberg	(313) 574-5814	AMSTA-TMC

DD FORM 1473, 84 MAR — 83 APR edition may be used until exhausted. All other editions are obsolete.

SUMMARY

The objective of the ceramic turbocharger rotor program was to establish the feasibility of producing a cost-effective ceramic rotor for the U.S. Army Tank-Automotive Command (TACOM). As part of the Manufacturing Methods and Technology Program, AiResearch Casting Company (ACC), as the major subcontractor, was to develop a manufacturing process to produce ceramic turbocharger rotors in production quantities.

Ceramic turbocharger rotors are of interest because the low density of the materials, compared to metals, produces about a 50 percent reduction in rotating inertia. This allows the turbocharger to accelerate faster and produce boost sooner which improves vehicle response. Also of interest is the elimination of costly and sometimes scarce metal elements since ceramics use abundant and low cost elements.

The ceramic rotor of this program is a replacement for the metal rotor of the Garrett Model TV81 turbocharger. This turbocharger is used on the military version of the Detroit Diesel Allison 8V92TA engine (rated at 460 bhp).

Silicon nitride was selected as the primary ceramic material from which to fabricate the rotors. An alternate, low-cost reaction-bonded silicon nitride was also studied in parallel during the early phase of the program. Slip casting was selected as the manufacturing process using the technology developed for the Automotive Gas Turbine (AGT 101 Program. Both "open-blade" and "closed-blade" techniques were considered. However, the latter was selected since it produced a net shape rotor and offered the only potential commercially viable and cost-effective process.

A total of 135 ceramic rotor castings were attempted. One hundred ten of the rotors were cast using the closed-blade process without yielding an acceptable rotor. At this point, a decision was made to revert back to the open-blade slip-casting process. A total of 25 rotors were attempted. Although the results were promising, it was apparent that further development still was needed that was beyond the scope and funding available in the program.

In summary, the design changes made to produce a ceramic rotor closer to near-net-shape to minimize machining changed the casting procedures and behavior previously observed in casting the ceramic rotors for the AGT101 Program. The design and casting modifications resulted in the inability to produce an acceptable, quality rotor.

In the interest of providing TACOM with an acceptable TV81 ceramic rotor turbocharger, Garrett began exploring other potential ceramic sources. Garrett has been actively working with a number of

Japanese ceramic suppliers over the past 5 years to develop ceramic rotors for passenger car and commercial diesel applications. The three principal suppliers, Kyocera, NGK Insulator and NTK Spark Plugs have excellent process capabilities, very good material properties and excellent facilities for producing both structural and net-shape ceramic components. U. S. ceramic suppliers such as Norton/TRW, GTE, Carborundum and Alcoa, etc., have experienced similar problems as ACC and have not been able to consistently produce acceptable net-shape ceramic rotors.

Although all three Japanese ceramic suppliers have demonstrated excellent net-shape capabilities, Kyocera was selected for the following reasons: 1) Utilizes a similar open-blade slip-casting process, 2) Consistently provided the best material properties and Weibull distribution, and 3) Demonstrated the ability to provide castings quickly.

A total of 25 TV81 ceramic rotors were received from Kyocera in late 1986. The ceramic castings were subjected to the standard Garrett Nondestructive Evaluation (NDE) inspection procedure. The ceramic rotors were then joined to the metal shaft and integrated into the TV81 turbocharger.

The following matrix of tests were successfully performed demonstrating the integrity of the ceramic rotor.

- Static Test-Test Bar
- Hot Spin Test
- Aerodynamic Performance Test
- Shaft Motion Test
- Durability Test

TABLE OF CONTENTS

VOLUME 1

TABLE OF CONTENTS (Continued)

LIST OF ILLUSTRATIONS

LIST OF ILLUSTRATIONS (Continued)

LIST OF ILLUSTRATIONS (Continued)

LIST OF TABLES

1.0 INTRODUCTION

This final technical report, prepared by the Garrett Automotive Group, Allied-Signal Corporation, for the U.S. Army Tank-Automotive Command (TACOM) under contract DAAE 07-85-C-R 147, describes the design and development of a ceramic rotor for the turbocharger (Model TV81) used on the military version of the Detroit Diesel Allison engine 8V92TA (rated at 460 BHP). The use of ceramic rotors, made from abundant and low-cost elements, eliminate the need for costly and sometimes scarce elements used in metal alloy rotors. Turbocharger rotating inertia is reduced by about 50 percent with the use of a ceramic rotor. This results in reduced time to boost for improved engine response and ultimately improved vehicle response.

2.0 OBJECTIVE

The objective of the ceramic turbocharger rotor program was to establish the feasibility of producing a cost-effective ceramic rotor for the U.S. Army Tank-Automotive (TACOM). As part of the Manufacturing Methods and Technology Program, AiResearch Casting Company (ACC), as the major subcontractor, was to develop a manufacturing process to produce ceramic turbocharger rotors in production quantities.

3.0 CONCLUSIONS

Ceramic rotors have been designed, produced and have successfully passed a series of acceptance tests.

Offshore ceramic suppliers have developed ceramic process capabilities and are able to produce near-net-shape ceramic turbocharger rotors. Both slip-casting and injection molding technicques have been successfully developed and are currently in production of ceramic rotors for passenger car turbocharger applications.

All major suppliers of ceramic rotors are of Japanese origin, namely: Kyocera Corporation, NGK Insulator and NGK Spark Plug. Domestic ceramic suppliers have not to date been able to successfully produce a "sound" ceramic casting for turrbcharger rotors.

The program objective for the development of a cost-effective manufacturing process for producing ceramic rotors could not be achieved. The cost of ceramic today is a major impediment to the widespread utilization of ceramics for automotive turbocharger applications. The cost of a turbocharger ceramic shaft wheel assembly is more than five times the cost of an equivalent metal shaft wheel assembly. Ceramic suppliers recognize the need to develop more cost-effective manufacturing techniques and processes and are currently working to achieve these objectives.

Material development has progressed to a level where silicon nitride ceramic rotors material strength and burst speeds are essentially equivalent to metal and have high-temperature capabilities up to and exceeding 1,000 C.

4.0 RECOMMENDATIONS

The ceramic rotor turbochargers furnished to TACOM from this program should be tested by TACOM for engine and vehicle response and also for durability.

If the ceramic rotor units show a significant performance improvement, TACOM should consider another program to develop a domestic source for ceramic castings. However, this program should be delayed until one or more domestic procedures demonstrates that they are very close to success.

5.0 DISCUSSION

5.1. Introduction

5.1.1 Program Scope. A contract was awarded to the Garrett Automotive Group (formerly the AiResearch Industrial Division, a division of the Garrett Corporation) by the TACOM in response to (RFP) No. DAAE07-85-R-R011 dated March 12, 1985. ACC was the major subcontractor.

The overall program shown in Figure 5-1 called for the ceramic rotor design activity (Phase One) to be completed within 3 months after contract startup.

Process development (Phase Two) was scheduled to begin initially using the existing TV8117 production metal rotor tooling. This was to provide the experience base for the slip-casting process until the final ceramic rotor tooling became available.

Fabrication of the ceramic rotor tooling and casting proceeded after receipt of contractor approval. Castings were scheduled to be available by the 8th month to allow shaft attachment activities to begin. Once the shaft assemblies were completed, the matrix of testing would begin. Testing included material specimen testing, hot spin test, shaft motion performance evaluation and durability testing.

5.1.2. Program Deliverables. The deliverable hardware items to be provided by Garrett are:

Fifteen ceramic rotors, as cast
Three finished shaft wheel assemblies
Two finished ceramic rotors
Three TV81 turbochargers

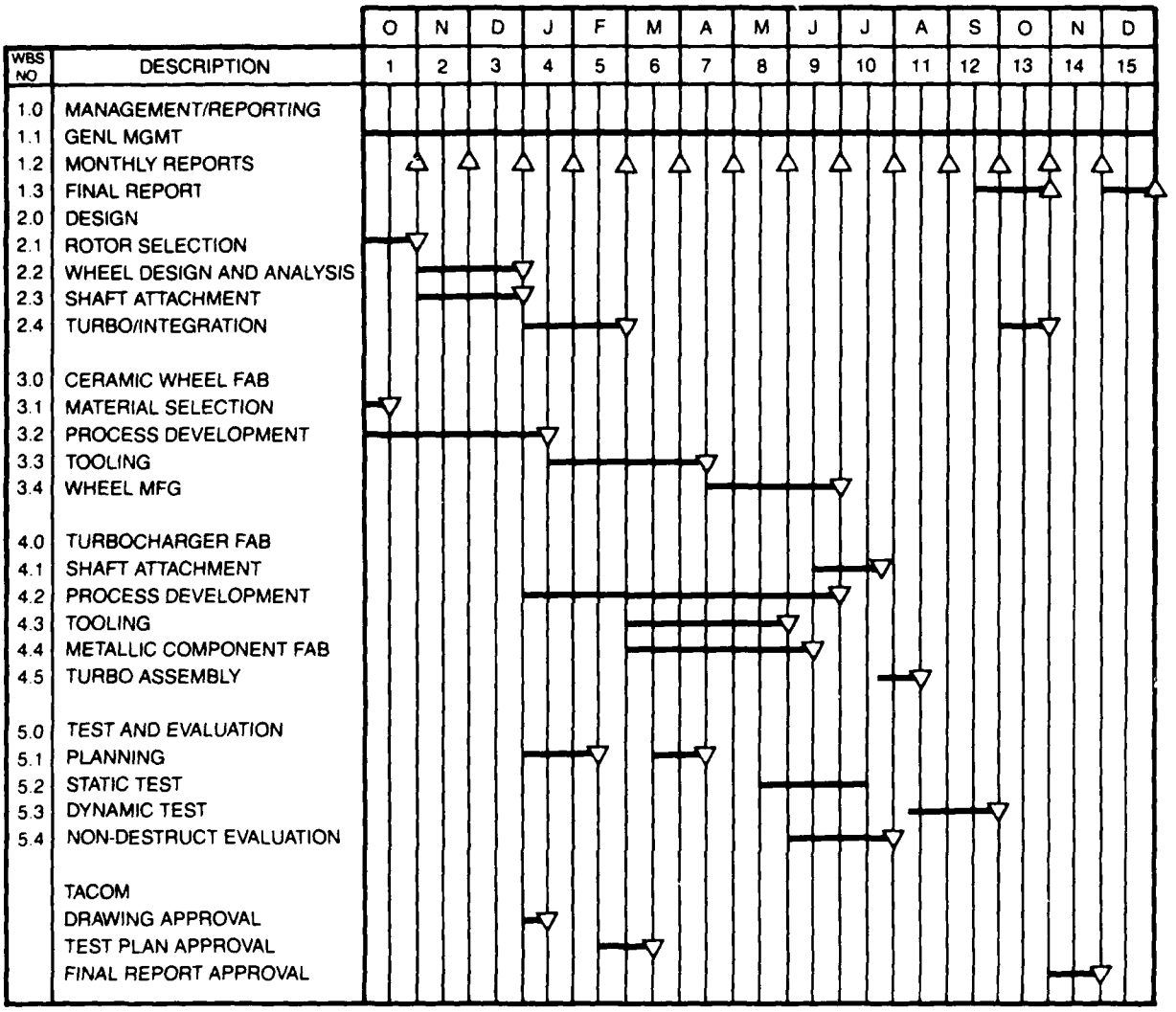

Figure 5-1. Program Schedule

5.2. Design Approach

5.2.1. Ceramic Rotor Design Methodology. The design and analysis of ceramic turbine wheels are guided by the special nature of ceramic materials. Unlike metals, in which plastic deformation mitigates the effects of flaws and stress concentrations, both of these items are of critical importance to the performance of ceramic components. Ceramics have both short- and long-term failure modes. In this design and analysis, the only failure mode considered was fast brittle fracture. In the design phase, special attention was given to reducing stress concentrations. In the analysis phase, a three-dimensional model was analyzed and a probability of success was calculated for the design condition. Statistical measurements of ceramic material properties are used in this calculation. Stresses due to thermal gradients are not considered in this analysis.

In evaluating the design of the wheel, the three main concerns are stress concentrations, resistance to foreign object damage (FOD) and total probability of failure. Because only test data has been available for judging resistance to FOD in terms of material strength and blade thickness, and not an exact equation, the blade thicknesses at the tip of the wheel are a result of engineering judgment at the start of the design. The backdisk radius has also been fixed by other constraints. The main constraint was the desirability to maximize interchangeable parts between units with metal and ceramic turbine wheels. The process of evaluating the design in terms of stress concentrations and total probability of failure proceeded as described below:

The preliminary design work used a two-dimensional finite element stress analysis which allowed changes in the design with a minimum of work. The effects on stress concentrations due to changes in blade thickness have been the primary emphasis at this stage. After an acceptable design has been achieved, a three-dimensional finite element was made and analyzed. The final step, calculating the total probability of failure, required the calculation of the probability of failure for each finite element using the Weibull distribution of the test bar data.

The starting point of the new ceramic turbine wheel design is the metal turbine wheel, assembly Part Number (P/N) 408492-14, and casting P/N 407545-2. The following are the overall results after the design work has been completed. The basic aerodynamic mean blade chord has not been changed nor have the hub and shroud contours. The only changes to the aerodynamic surfaces are a new blade thickness distribution and new angle between the trailing edge and the hub line. The new angle is 86 degrees, compared to 90 degrees, a four-degree change. The trailing edge has been rotated four degrees about its midpoint. Previous performance studies show no significant changes in performance until a seven-degree change

in angle. The change in blade thickness distribution is necessary to reduce the stress concentration at the blade root radius. In the throat area of the blade channel, the blade thicknesses are nearly identical and, therefore, no change in flow is expected.

A comparison of mechanical characteristics between the metal wheel and a ceramic wheel listed below shows the ceramic wheel to be as good or better than the metal wheel in most respects. In weight and polar moment of inertia, the clear advantages of ceramics for transient engine response can be seen.

COMPARISON OF MECHANICAL PROPERTIES

	Metal	Ceramic
Wheel Assembly Weight (lbs)	2.75	1.33
Tip Diameter (in)	4.385	4.385
Exducer Diameter (in)	3.822	3.822
Exducer Natural Frequency (Hz)	5,650	8,650*
Tip Natural Frequency (Hz)	6,990	17,800*
Polar Moment of Inertia (in-lbs-sec^2)	.00574	.00229
Average Burst Speed (r/min)	126,000	140,000*

*Calculated

In the beginning of the project when actual material data was not available, a set of minimum properties was picked as the basis of the design. These properties are shown below. The design of the the wheel was based on these properties. After the change in wheel casting vendors, a new set of properties was added for the final performance calculations also shown below. No significant changes in the physical dimensions of the wheel would be expected if the wheel were redesigned with the new properties from the beginning. The increased material and Weibull modulus only adds to the burst speed and resistance to FOD.

MECHANICAL PROPERTIES OF CERAMICS

	Design Material	Kyocera SN220M
Density (lbs/in^3)	.118	.115

Modulus of Elasticity (psi)	42.5×10^6	42.5×10^6
Poissons Ratio	.30	.28
R. T. Characteristic 4 Point Bending Strength (ksi)	96	115
Weibull Modulus	8.7	13.5
Coeff of Thermal Expansion (in/in°F)	1.83×10^{-6}	1.83×10^{-6}

5.2.2. Ceramic Rotor Two-Dimensionsl Analysis. A final series of two-dimensional analyses have been done to check the new design changes. The Garrett finite element program, called ISOPDO, has been used for both plane and axisymmetrical types of analysis. The axisymmetrical analysis naturally uses the section along the axis of rotation. The model for the TV81 ceramic turbine wheel consists of 167 elements and 192 nodes as shown in Figures 5-2 through 5-5. Only stresses from rotation at 80,000 r/min are shown. Only stresses in the hub section are correct as the blade stresses can not be accurately modeled in two-dimensional sections of this type. The maximum principal stress is 18,900 psi.

The stresses in the blade and blade fillet area are best modeled in a two-dimensional section by a plane section perpendicular to the axis of rotation. This model consists of 104 elements and 130 nodes as shown in Figure 5-6. The plot of maximum principal stress is shown in Figure 5-7. Analysis of this plane section shows a 30-percent reduction in peak stress at the blade root from the original design. No effects of blade bending were modeled in this section.

5.2.3. Ceramic Rotor Three- Dimensional analysis. In order to define the statistical characteristics of the design, a three-dimensional analysis of the complete wheel is required. Because of the symmetrical nature of the wheel, only a sector of the wheel containing one blade is needed to model the entire wheel. The mesh generator sections of the computer program, RATRAP, has been used to create the basic three-dimensional model. This model has been transferred to another computer program, ANSYS, for further model refinement. The blade root fillet sections have been hand modified to conform to the real wheel. Solid 8 node brick elements are used to model both the blade and hub sections of the wheel. In the blade, two thicknesses of elements are used, while six thicknesses of elements are used in the hub. The model is seen in Figure 5-8. This model consists of 664 elements and 1,187 nodes. The elements have been arranged so the free surface stresses can be used in calculating the probability of failure.

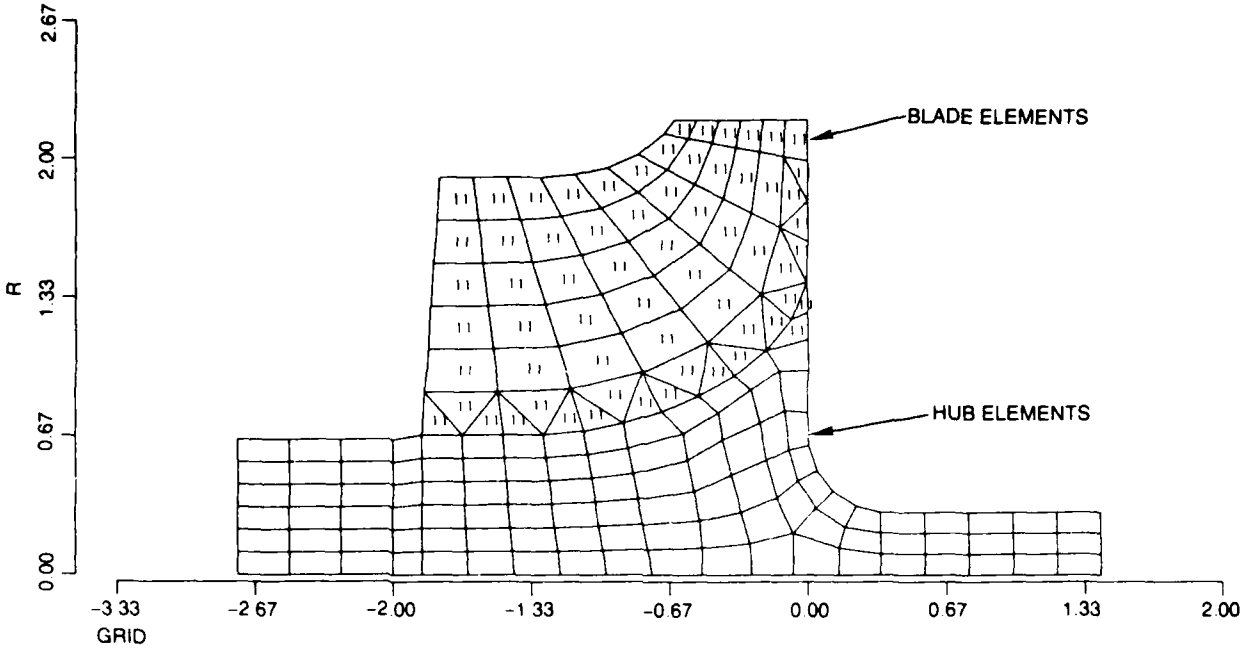

Figure 5-2. Element Mesh for Axisymmetric Model

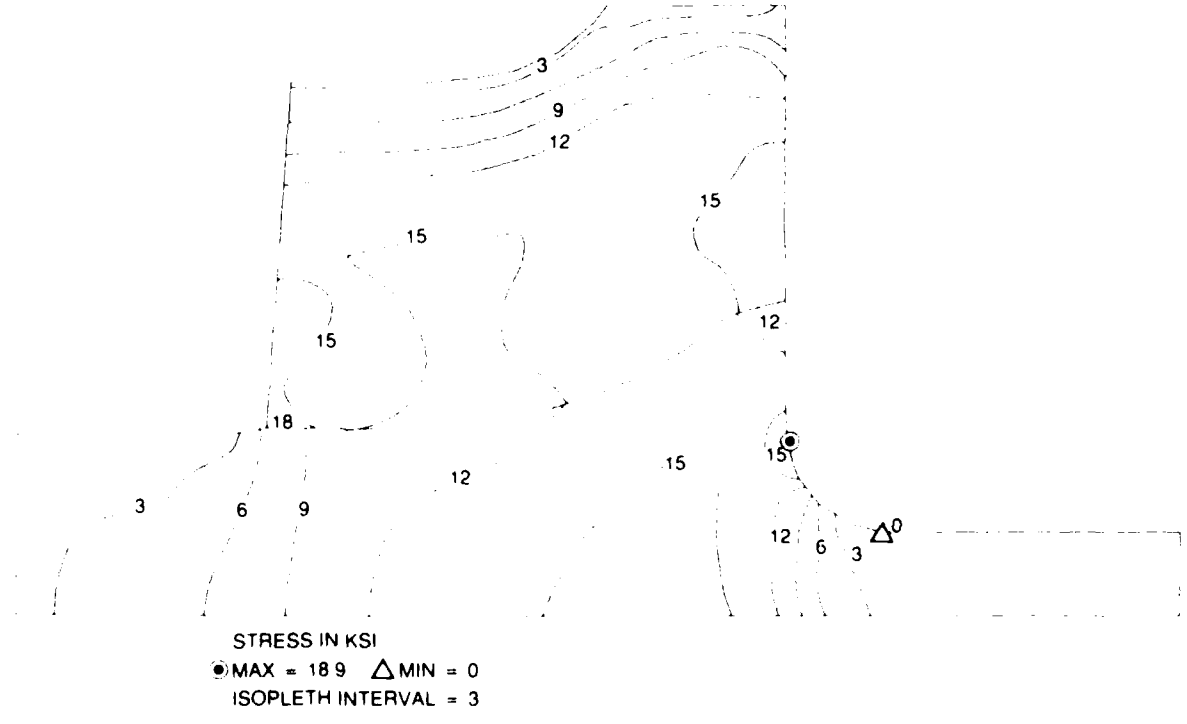

Figure 5-3. Maximum Principal Stress

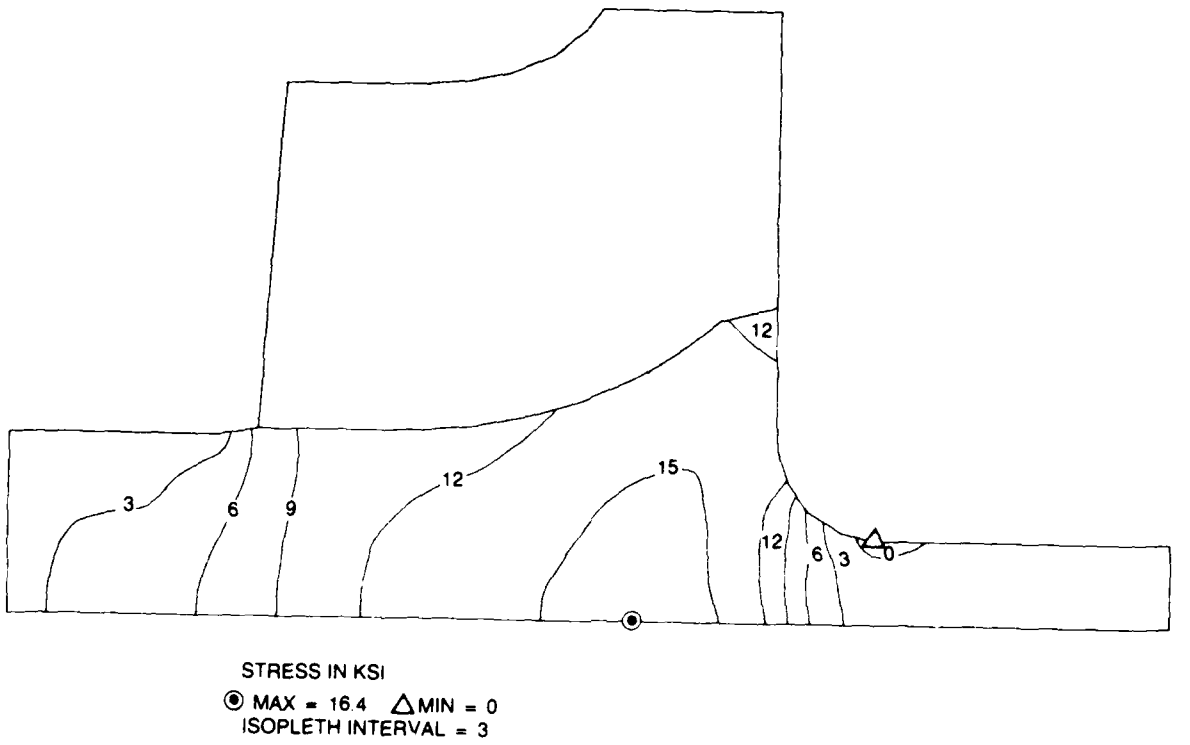

Figure 5-4. Tangential Stress

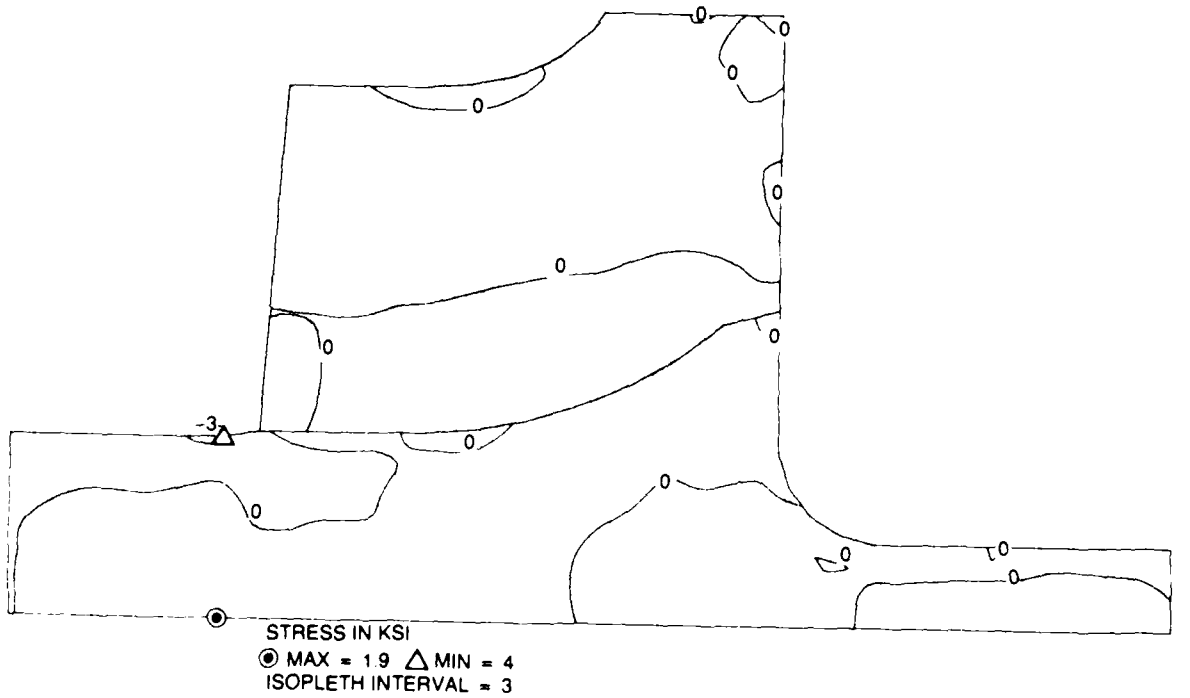

Figure 5-5. Minimum Principal Stress

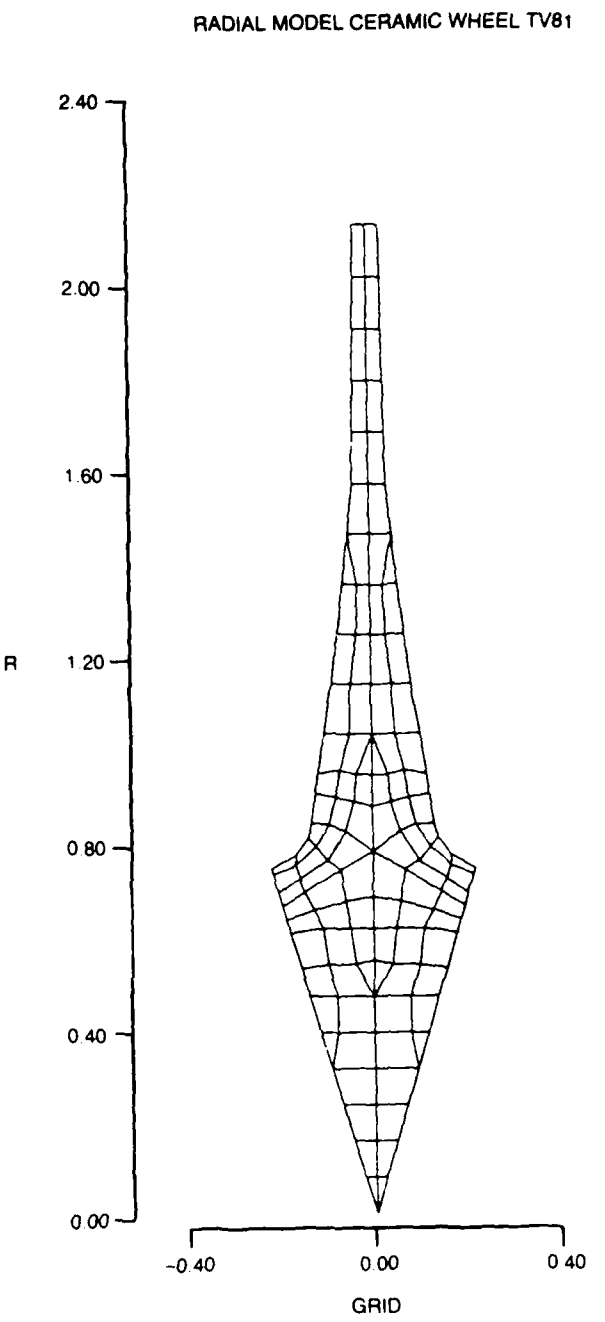

Figure 5-6. Grid for Radial Model

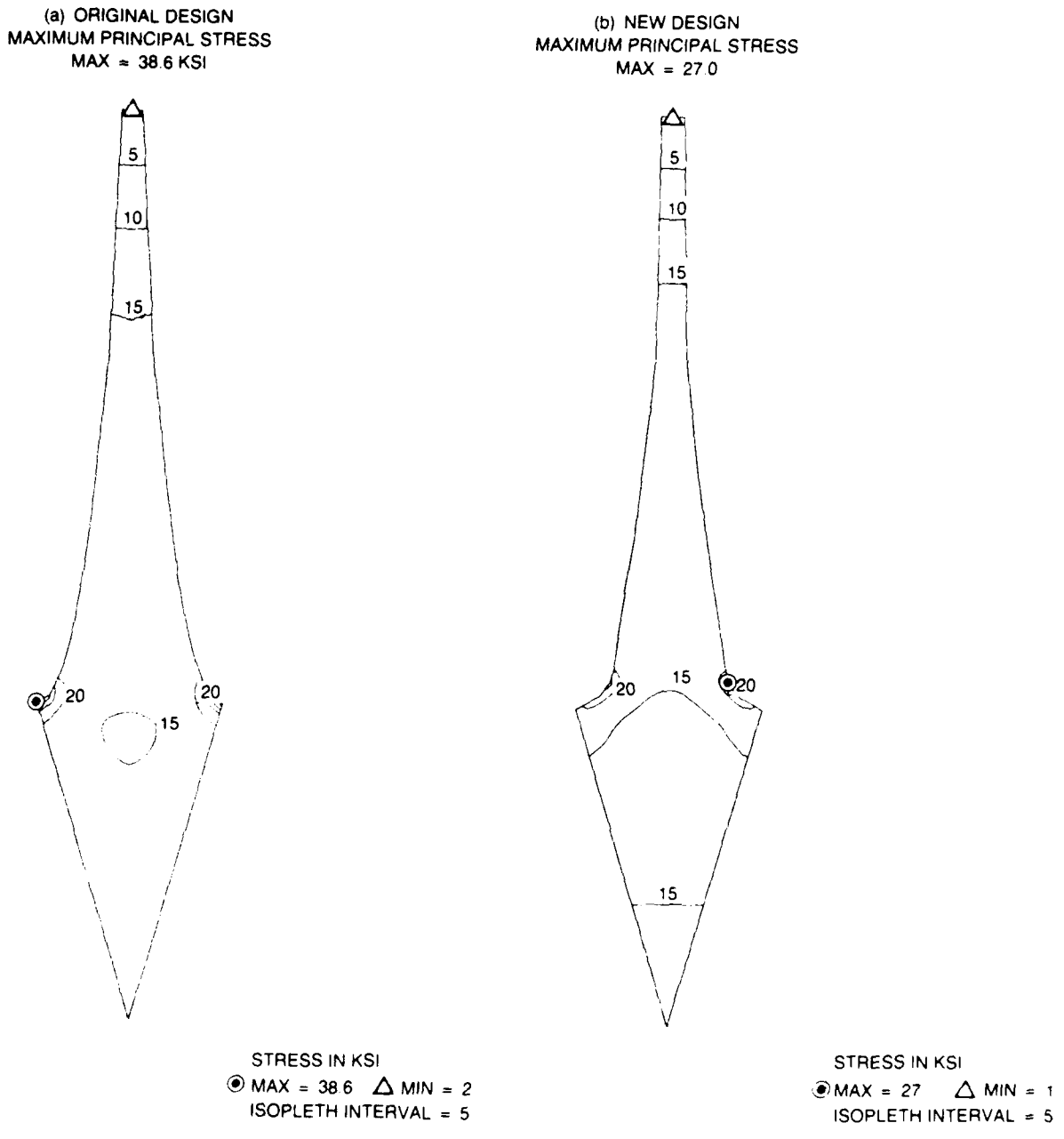

Figure 5-7. Maximum Principal Stresses

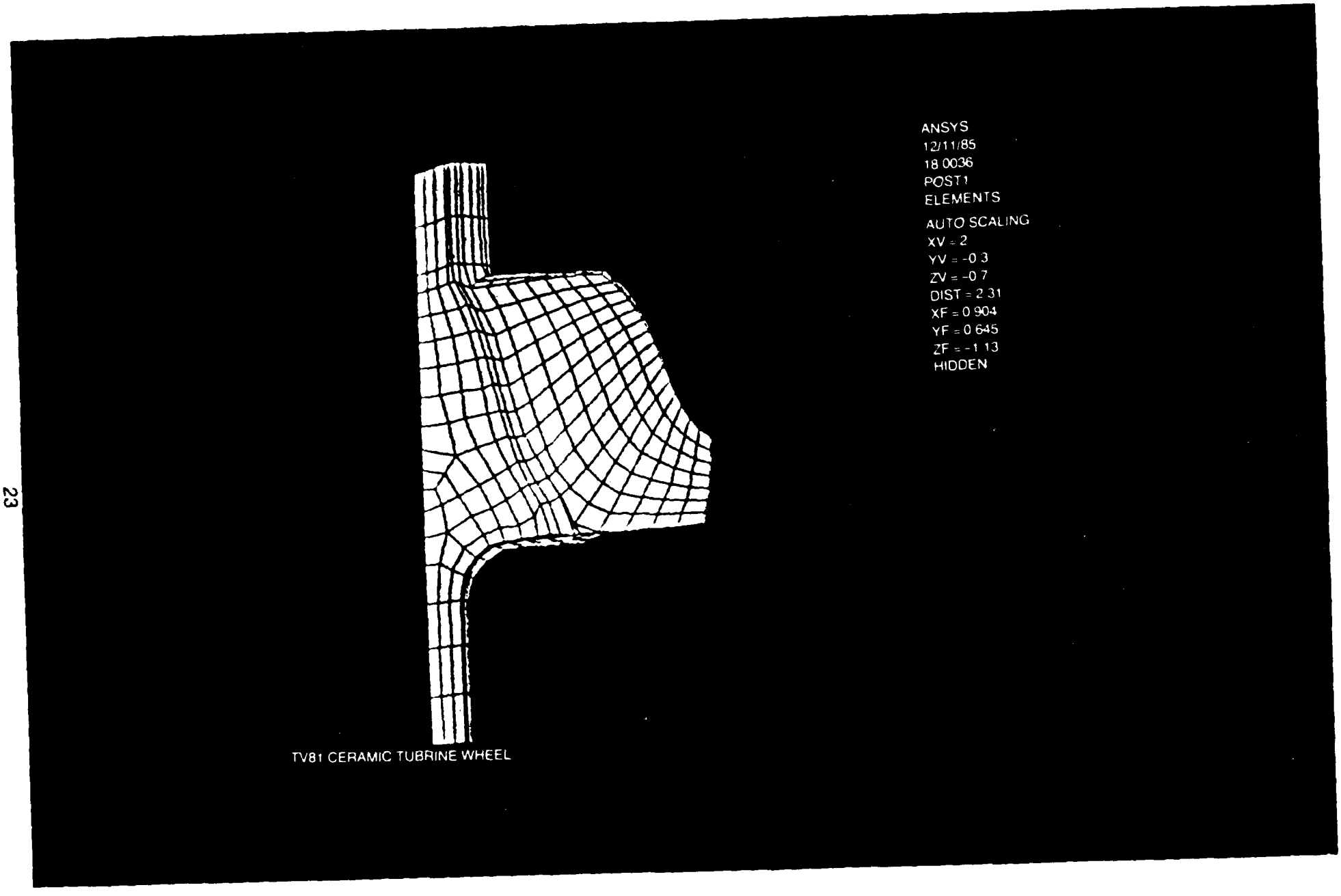

Figure 5-8. Cathode Ray Tube (CRT) Display of Three-Dimensional (3-D) Model

The analysis has also been done using the ANSYS program. The conditions of the analysis are for uniform temperature of 21 °C (70 °F) and a turbocharger speed of 80,000 r/min. Also included in the analysis is the compressive pressure on the shaft from the shrink fit of the shaft attachment. No aerodynamic loads are imposed on the blades.

The stress plots from the results of the analysis are shown in Figures 5-9 and 5-10. The plots are of the maximum principal stress. The maximum stress, which occurs at the blade hub intersection, is about 24,000 psi as seen in the largest red area of Figures 5-9 and 5-10. This area is only a moderate stress concentration and fairly small. A very small additional red area can be seen in Figure 5-10 at the blade hub backface intersection. The axial curvature of the blade causes a bending action in the blade. This effect can be seen by observing the large high stress yellow area in the blade of Figure 5-10 and the lower stress green area on the opposite side of the blade in Figure 5-9.

The dark blue area in the shaft denotes the compressive stresses from shrink fit of the shaft attachment. The values shown are maximum principal stress. The greatest compressive stress, i.e. the minimum principal stress, in the shaft is 18,000 psi.

5.2.4. Weibull Analysis. The analysis is completed by finding the probability of failure for the three-dimensional analysis conditions. The statistical data gathered from breaking the test bars is combined with the results of the three-dimensional analysis. A characteristic strength and Weibull modulus for both the surface and the volume of the test bar are found. The stresses in each element of the model are compared to the test bar data, and a probability of success is calculated. From these probabilities, a total probability of success and failure is calculated. The probability of failure due to both surface and internal flaws are calculated. The expression for this integration is shown in Figure 5-11. A computer program, ANSTAT, has been used to complete the calculations. ANSTAT uses the principal stresses as calculated by ANSYS at centroid of the volume and also at surface of an element when required. The Weibull distribution for the total probability of failure is shown in Figure 5-12. The design material is calculated to have a .1-percent failure rate at 80,000 r/min while the Kyocera SN220M material is calculated to have the same .1-percent failure rate at 100,000 r/min.

For the TV81 wheel, 5 percent of the failures are expected to be from surface flaws, 95-percent from internal flaws. (Note: these flaws are microscopic in nature.) The 19 most highly stressed elements out of 664 elements are responsible for over 30-percent of the probability of failure. The effects of stress concentrations become greater as the number of material flaws become smaller as expressed by the increase in the Weibull modulus. All of

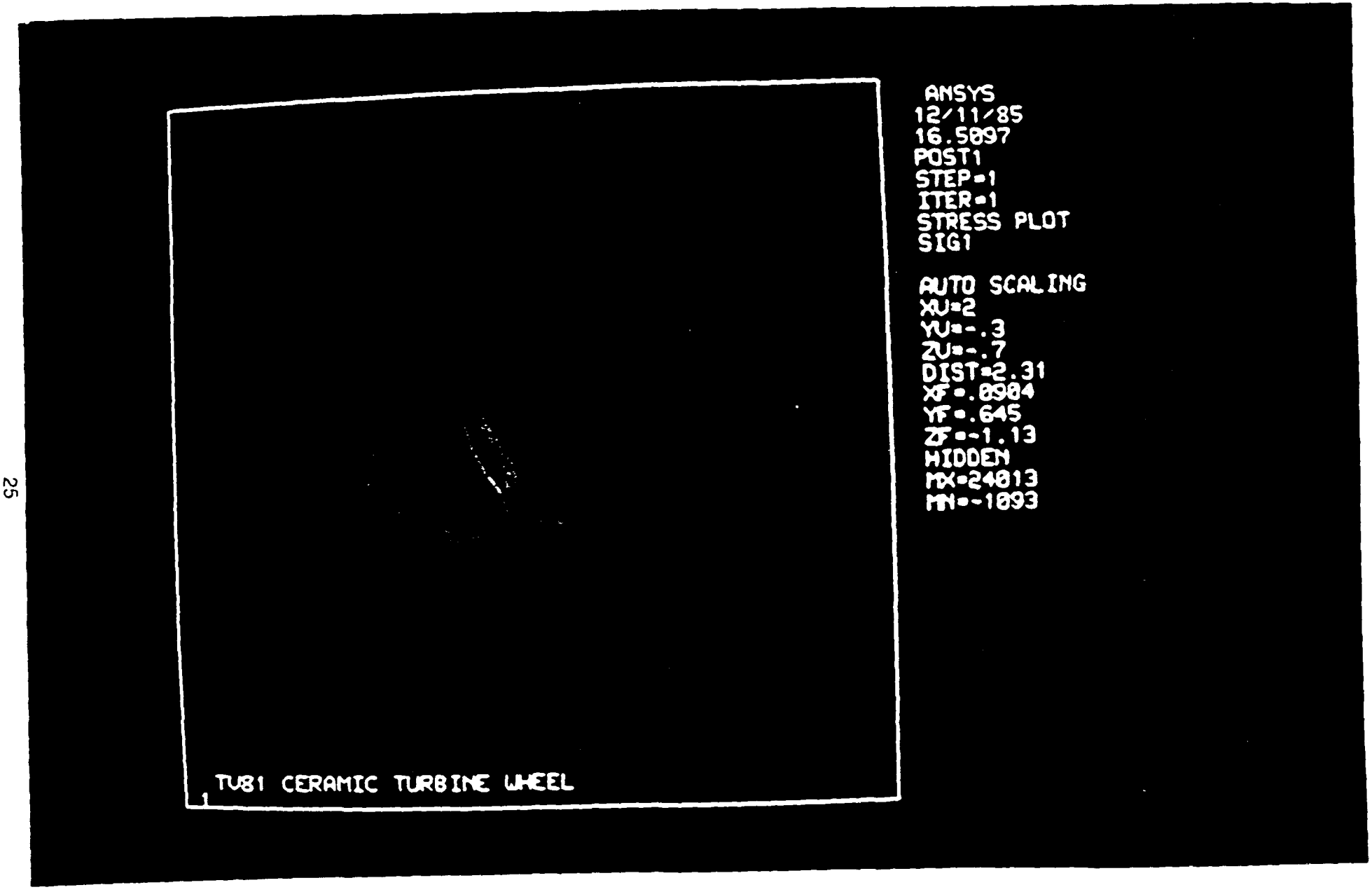

Figure 5-9. CRT Display Showing Maximum Principal Stresses (Stress in KSI)

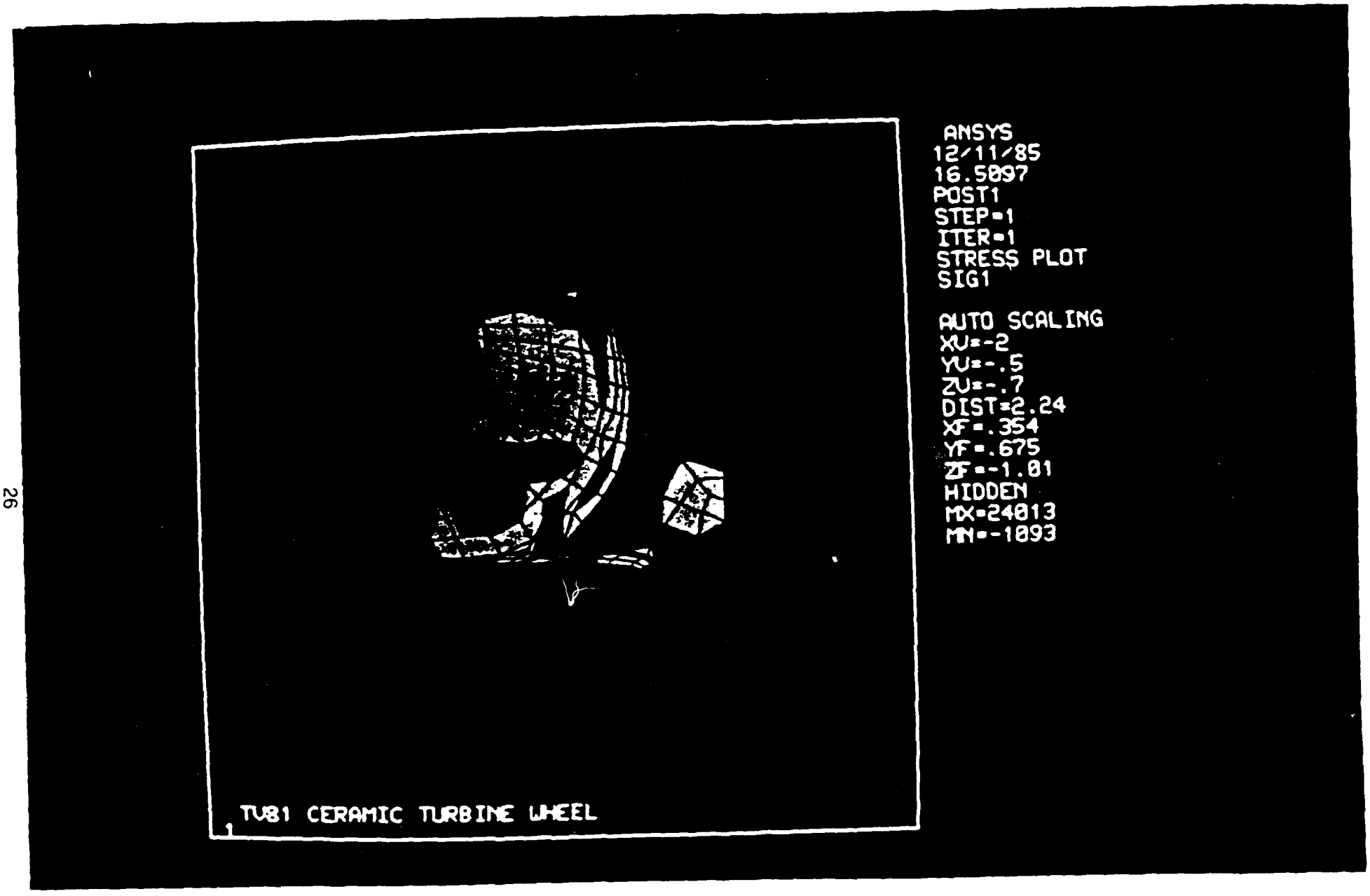

Figure 5-10. CRT Display Shows Acceptable Stress Pattern In Ceramic Rotor Blade

$$P_{vi} = \text{EXP}\left[(-1) * \left(\sum_{j=1}^{3} \left(\frac{\sigma_{vj} - \sigma_{ov}}{\sigma_{cv}}\right)^{M_v} * \left(\frac{V_i}{V_T}\right)\right)\right]$$

$$P_{si} = \text{EXP}\left[(-1) * \left(\sum_{j=1}^{3} \left(\frac{\sigma_{sj} - \sigma_{os}}{\sigma_{cs}}\right)^{M_s} * \left(\frac{A_i}{A_T}\right)\right)\right]$$

Total Probability of Volume Success $(P_{vt}) = \prod_{i=1}^{n} P_{vi}$

Total Probability of Surface Success $(P_{st}) = \prod_{i=1}^{n} P_{si}$

Total Probability of Combined Failure = $1 - (P_{vt} * P_{st})$

P_{vi} = Volume Element Probability of Success
σ_{cv} = Volume Characteristic Stress
M_v = Modulus for Volume Characteristic Stress
σ_{vj} = Principal Stress at Centroid of Stress Element
V_i = Volume of Stress Element
V_T = Volume of Test Bar
σ_{ov} = Volume Minimum Stress
P_{si} = Surface Element Probability of Success
σ_{cs} = Surface Characteristic Stress
M_S = Modulus of Surface Characteristic Stress
σ_{sj} = Principal Stress at Centroid of Stress Element Face
A_i = Surface Area of Stress Element Face
A_T = Surface Area of Test Bar
σ_{os} = Surface Minimum Stress

Figure 5-11. Mathematical Expression for the Calculation of the Probability of Success or Failure of a Ceramic Rotor

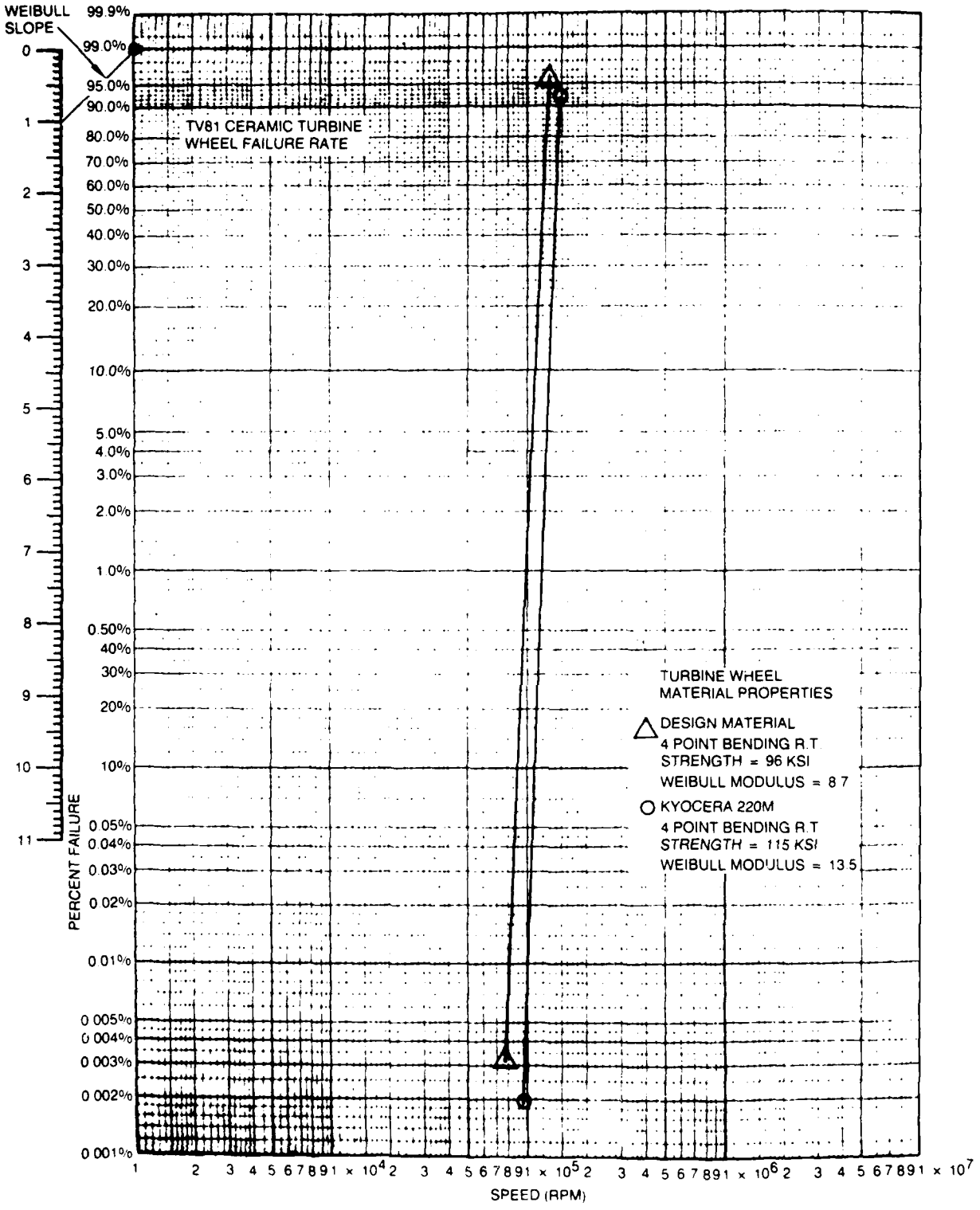

Figure 5-12. Turbine Wheel Material Properties

the above probabilities are calculated on the basis of failure due to fast fracture of the ceramic with short-term exposure to the analysis conditions.

There are several reasons for the use of fast fracture as the sole design criteria for this type of design at this stage of ceramic technology. First, fast fracture is a major mode of failure. Fast fracture is the mode of failure in burst tests. The strength of the ceramic in fast fracture is the starting point for determining failure by slow crack growth. The probability of failure at a given time can be given as a factor of the probability of failure from fast fracture for a given stress condition. With the rapid change in the improving properties of ceramics, long-term properties of the best ceramics are not available. With time and a greater amount of property data on acceptable materials, a broader analysis will include both short- and long-term phenomenon. Proven failure criteria for the triaxial stress state is now nearly developed. Especially important will be the analysis of foreign object damage.

5.2.5. Ceramic Rotor Material Selection. The objective of the program was to develop a cost-effective manufacturing process for producing ceramic turbocharger rotors in production quantities. Silicon nitride was selected as the primary ceramic material from which to fabricate the rotors. The material systems used were based on following formulations:

- Code 1 Formulation:

  - GTE SN-502 or H.C. Starck H-2 Silicon Nitride
  - Yttrium Oxide (8% by weight)
  - Aluminum Oxide (4% by weight)

- Code 2 Formulation:

  - GTE SN-502 or H. C. Starck Silicon Nitride
  - Yttrium Oxide (6% by weight)
  - Aluminum Oxide (2% by weight)

An alternate, low-cost reaction-bonded silicon nitride was studied in parallel with the baseline silicon nitride. The material designated code 27 formulation was similar to the Code 2, except that the base material used is a combination of the silicon metal and silicon nitride powder instead of silicon nitride exclusively.

5.2.6. Ceramic Rotor Process Selection. The basis of having a successful TACOM rotor program was founded on being able to transfer and utilize the slip casting technology developed from the AGT-101 program. Since cost-effectiveness was the second major objective of the program, an economical, near-net-shape fabricating process was also necessary. Injection molding was considered since

it offered the capability of achieving a near-net-shape rotor. However, the cost of producing injection tooling for the limited number of rotors needed would have been prohibitive. Using the AGT-101 slip-cast rotor fabrication techniques and a closed-blade mold design was expected to result in acceptable ceramic rotors.

Three key factors influenced the decision to concentrate on the single approach in developing a manufacturing process: 1) The need to produce deliverable rotors using the process developed in the program within a very short time necessitated an early decision as to the process selected. 2) Available funding precluded the development of more than one process. 3) A process that produced as close to a net-shape rotor offered the only practical approach to achieving a commercially viable and cost-effective process.

5.2.7. Ceramic Rotor Process Description. Slip casting is initiated with the preparation of raw materials (see Figure 5-13). Silicon nitride (Si_3N_4) powder is milled with set percentages of yttrium oxide (Y_2O_3) and aluminum oxide (Al_2O_3) (used as densifying aids during sinter-HIP) in a rubber-lined mill with silicon nitride media. The powder is milled to a particular particle size that will allow for good slip rheology (low viscosity, high specific gravity, stable pH) and a high green density when the milled powder is made into a slip and cast into a rotor.

Once milled, the powder is mixed with water into a slurry or slip. Enough water is added to maintain good viscosity while having as high a green density as possible. The slip is allowed to outgas and stabilize in viscosity from 4 to 5 days. During the "aging" period of the slip, organic deflocculents and stabilizers are added (if needed) to obtain and/or maintain proper viscosity (100 to 300 centipoise) and green density (2.05 to 2.15 g/cc).

In the meantime, wax and plaster mold preparation can take place. Using the TACOM rotor as the example, the actual rotor fabrication begins with the injection of water-soluble wax into patterns (Figure 5-14 left). From soluble wax injection, the wax pattern is assembled onto a tooling fixture and dipped in an insoluble wax (see Figure 5-15). The wax assembly is machined to trim off excess wax and to allow the wax shell to fit properly onto a plaster. Once machined, the wax pattern (see Figure 5-14, right) is soaked in water to completely dissolve the soluble wax pattern. The wax shell is then mounted onto a plaster (Figure 5-16) designed specifically for the machined wax shell. An alignment fixture (see Figure 5-17) is used to hold the shell in place on the plaster, allowing the symmetry of the rotor (formed by the wax shell) and the rotor shaft (formed by the plaster) to be maintained (Figure 5-18 shows assembled mold).

When the properties of the silicon nitride slip are proper, the slip is screened (100 mesh screen), de-aired and poured into the mold assembly while the assembly is mounted on a spinning

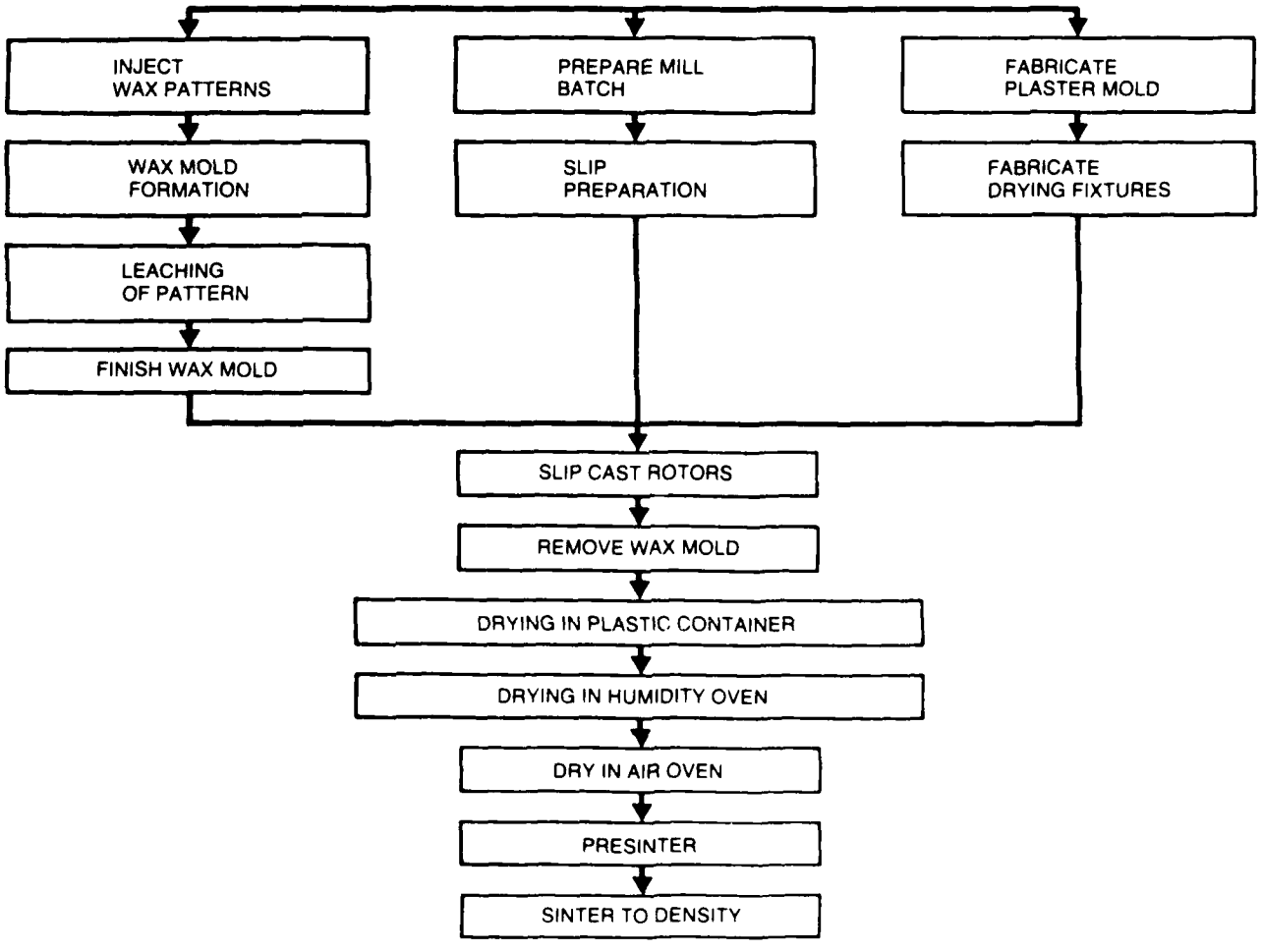

Figure 5-13. Flow Chart Showing Slip/Casting Process

Figure 5-14. Revised TACOM Injection Wax Pattern (Left), Complete TACOM Wax Shell (Right)

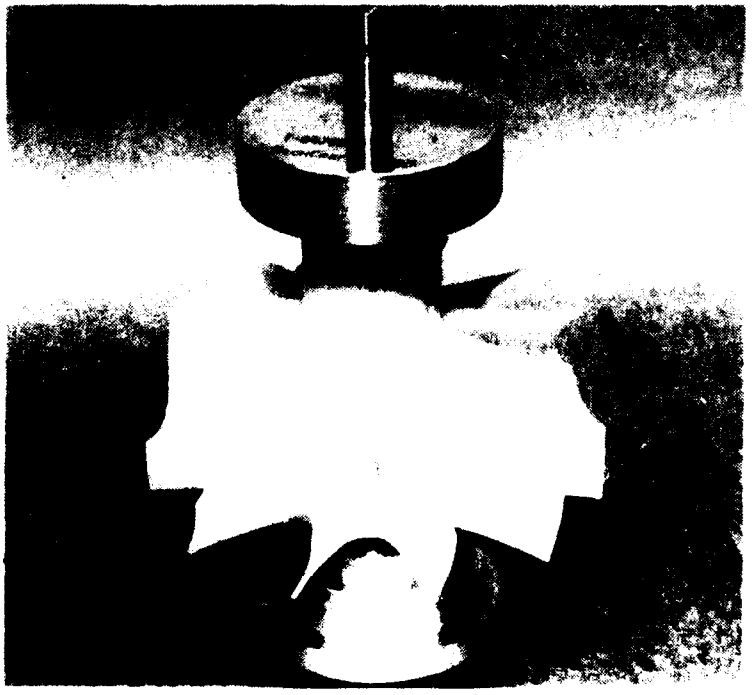

Figure 5-15. Revised TACOM Wax Pattern Mounted in Wax Dipping Fixture

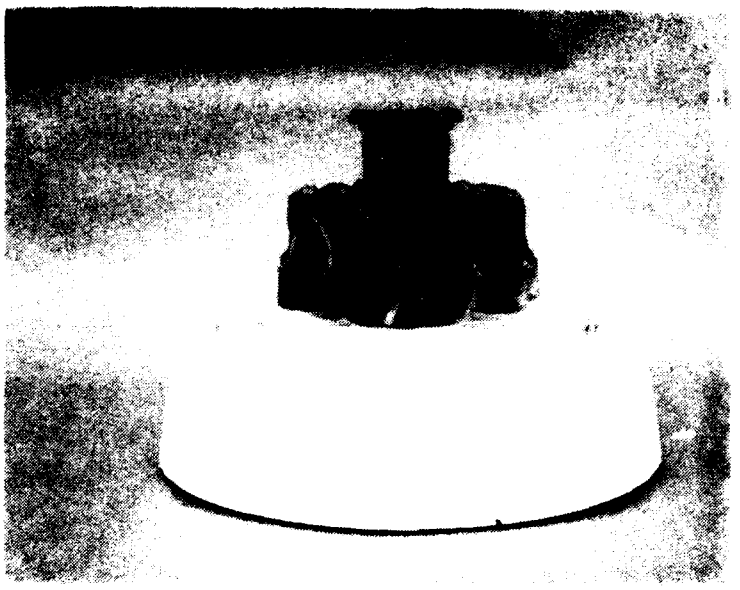

Figure 5-16. Revised TACOM Wax Shell Mounted on Plaster Mold

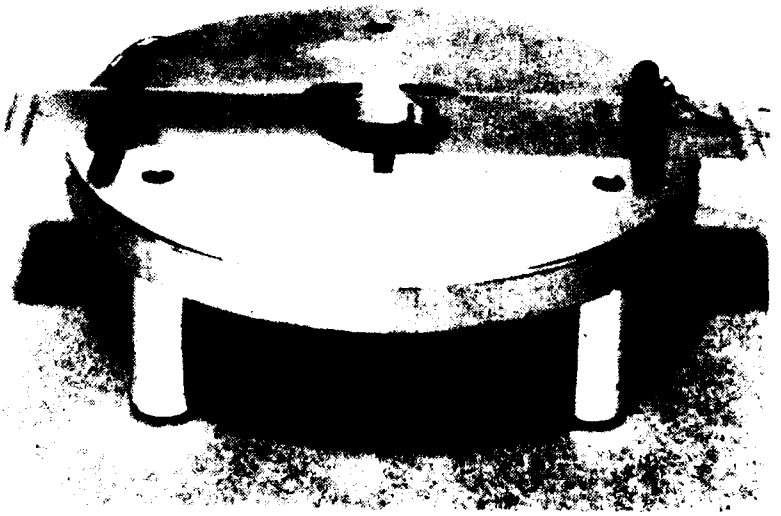

Figure 5-17. Alignment Fixture for Plaster Mold Assembly

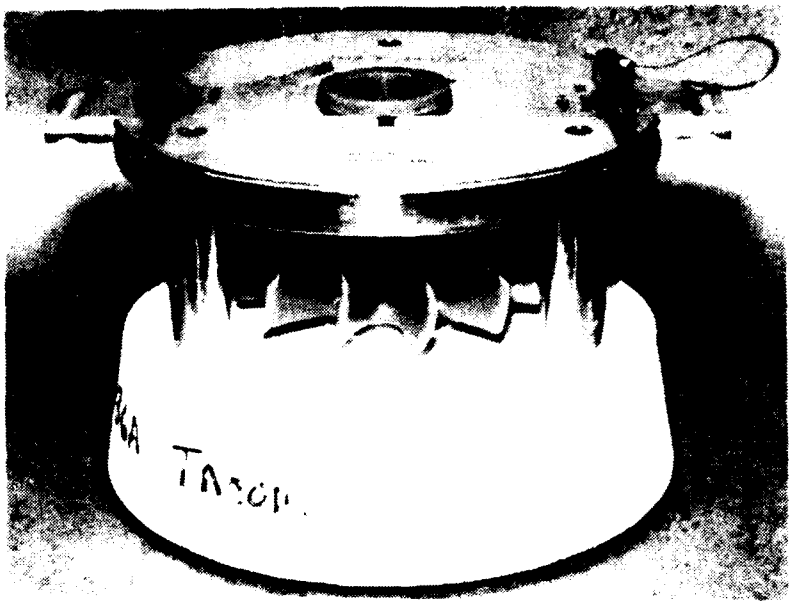

Figure 5-18. Complete TACOM Mold Assembly

Figure 5-19. Green TACOM Rotor (Revised Design)

turntable. The turntable is used to centrifugally force slip into the blades to assure complete blade fill. Once the slip completely fills the mold, the rotor assembly is placed in a humidity chamber until the rotor has completely cast (3 to 4 days). The rotor is then removed from the plaster base.

To remove the wax shell from the cast rotor without damaging the rotor, the wax is chemically removed in a solvent that does not harm the ceramic rotor. The green rotor (see Figure 5-19) is dried slowly (2-3 days) in air to prevent drying cracks, followed by humidity-controlled drying (up to 90 ^{o}C) and oven drying (110 ^{o}C). When drying is complete, the rotor is processed in a presintering furnace at 1400 ^{o}C (1-day cycle) to partially densify and strengthen the rotor. The rotor is then sinter-HIP'ped (Hot Isostatic Processed) for a 1- day cycle at 1,800-1,900 ^{o}C and 30 ksi pressure. (Figure 5-20 shows a presintered and a sinter-HIP'ped rotor: Figure 5-13 shows an outlined summary of the process steps).

5.2.8. Ceramic-to-Metal Joint. A number of ceramic-to-metal joints have been successfully developed for turbocharger applications. These joints range in design from shrink fits, active braze joints, butt joints using compliant metal layers and press fit joints. Because of the differences in thermal expansion of ceramic to metal, radial and axial stresses are unavoidable at the joint interface. A rigorous theoretical design analysis as well as extensive experimental tests were necessary to design for the torsional and bending loads under cyclic and thermal loads.

The Garrett ceramic-to-metal joint consists of an incoloy sleeve which is mechanically press fitted to the ceramic stub shaft which is then brazed to the 4140 shaft. The joint is designed to withstand the necessary torsional bending loads and thermal cycling.

The ceramic shaft wheel assembly is shown in cross-section in Figure 5-21 and in photographs in Figures 5-22 and 5-23.

5.2.9. Turbocharger Design Modifications. Only three parts of the turbocharger assembly required modification to accept the ceramic turbine wheel. Those parts are the turbine side journal bearing, the turbine side bearing wear washer and the wheel shroud. See Figure 5-24.

The standard TV81 journal bearing inside diameter was enlarged from .6272/.6268 inches to .7018/.7014 inches to fit the larger diameter shaft wheel assembly. The same shaft-to-bearing clearance was maintained.

Enlarging the inside diameter of wear washer P/N 407135 from .650/.670 inches to .730/.750 inches gives the necessary clearance for use against the turbine side bearing.

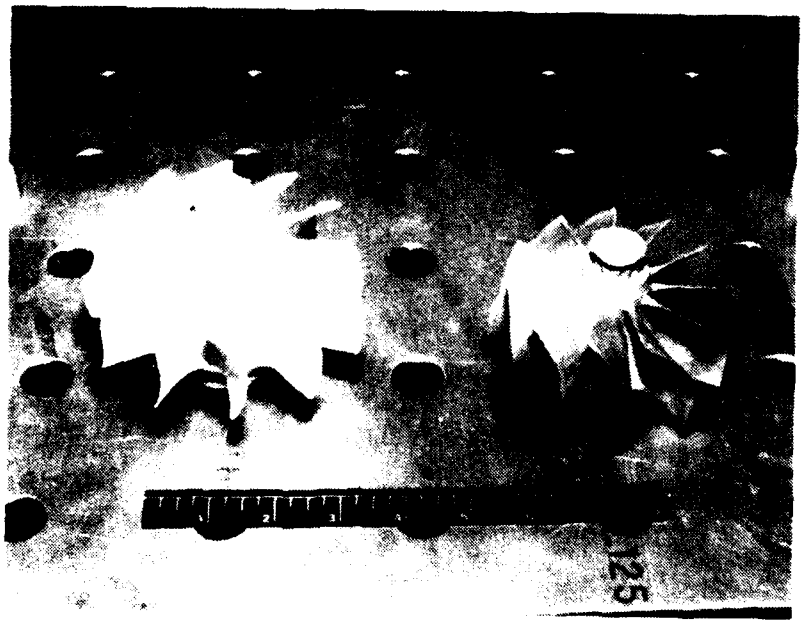

Figure 5-20. Presintered TACOM Rotor (Left), Sintered TACOM Rotor (Right)

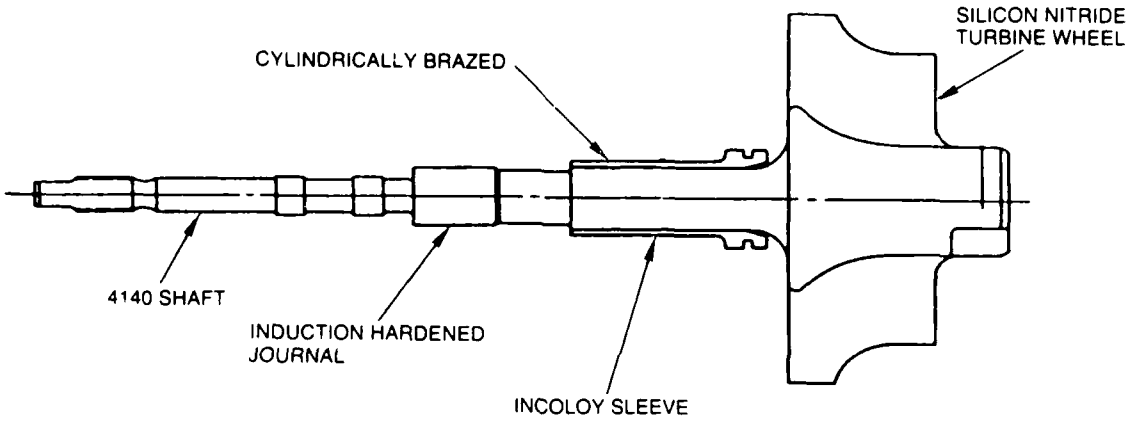

Figure 5-21. Ceramic Shaft Wheel Assembly

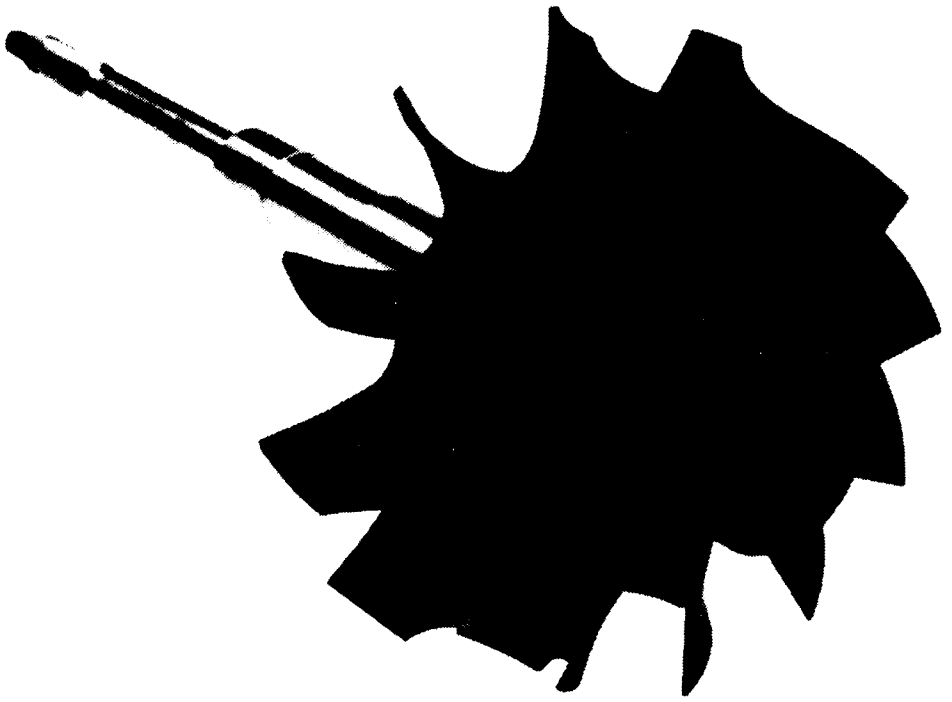

Figure 5-22. TACOM TV81 Ceramic Shaft Wheel Assembly

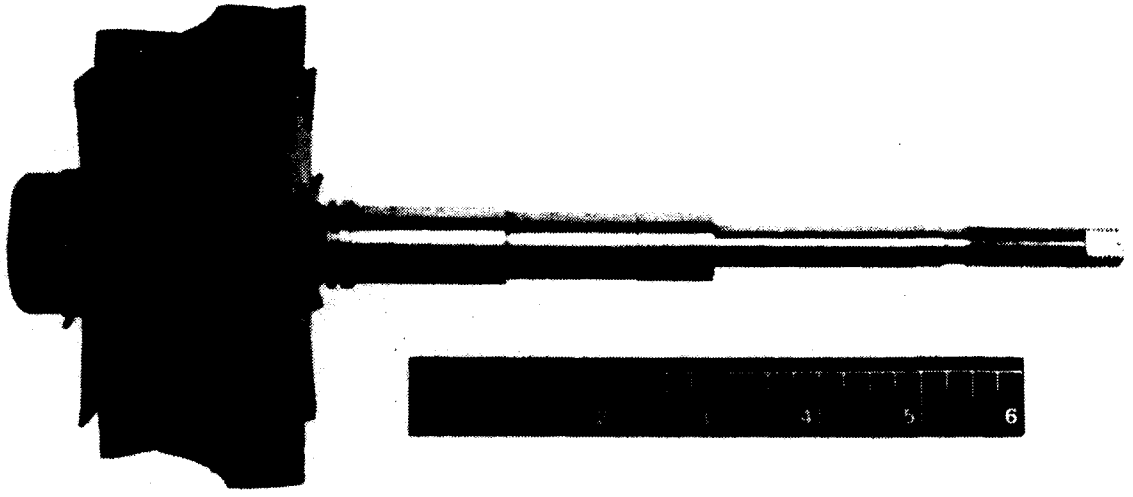

Figure 5-23. TACOM TV81 Ceramic Shaft Wheel Assembly

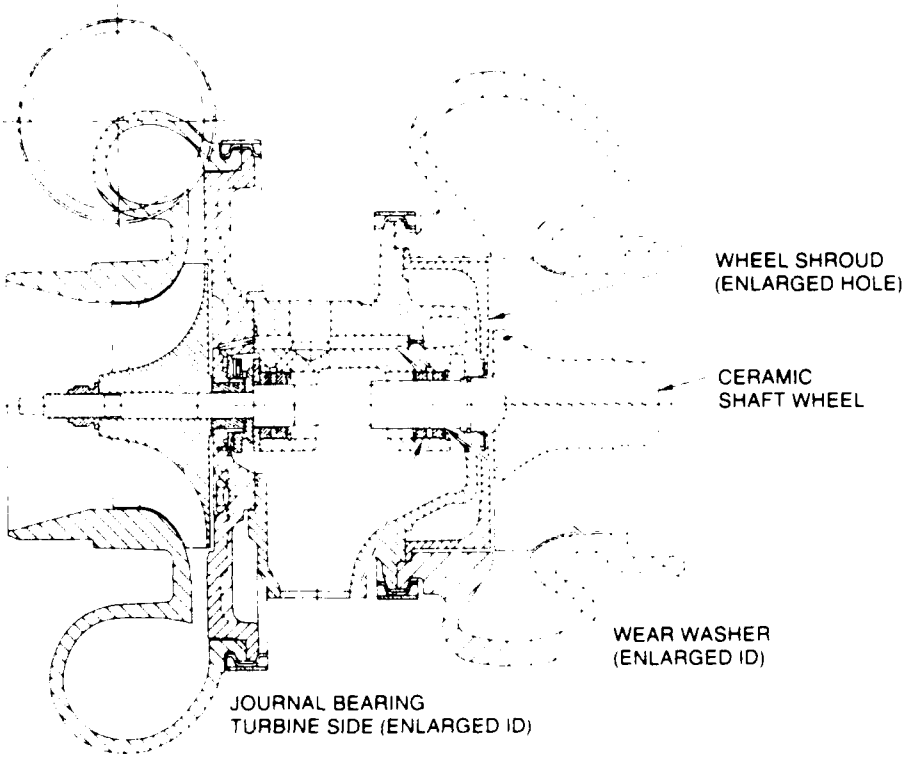

Figure 5-24. Design Modifications to Accommodate Ceramic Shaft Wheel in TV81

The ceramic turbine wheel has a much larger blend radius from the wheel back-disc to the stub shaft than the same feature on the metal wheel, plus the ceramic shaft is larger in diameter in this same area. These differences cause an interference between the wheel and the shroud. To correct this problem, the size of the hole in the shroud was enlarged from .860/.865 inches to 1.000/1.005 inches.

The complete parts list for both the ceramic wheel unit and the metal wheel unit are shown in Appendix A.

5.3. Ceramic Rotor Fabrication - Original Program

ACC was selected as the major sub-contractor to produce the ceramic rotors. Process development began using existing, production TV8117 metal rotor tooling. This provided the experience for the slip-casting process until the final ceramic wheel design was available.

Fabrication of the rotor-casting tooling and ceramic rotors followed. Schedule of the program activities are shown in Figure 5-25.

Following is a summary of the ACC development activities:

5.3.1. Phase One(Metal Blade Tooling). In Phase One, initial fabrication used the TV8117 metal turbocharger rotor design. To form the metal blade configuration, a wax injection die pattern used to form wax patterns for the metal rotor used to create the water-soluble wax patterns for the eventual ceramic rotor (Figure 5-26, left). The soluble wax pattern would be dipped in a nonwater soluble wax. The pattern would be placed in water to dissolve the encased soluble wax pattern, leaving a wax shell. The wax shell would be aligned to a plaster mold base configured to form the rotor shaft. The combined wax/plaster assembly was the basic method to form the TACOM rotor (Figure 5-26, right). Rotors cast using the TV8117 configuration were analyzed to determine final density and shrinkage factors necessary to design the modified tooling. More importantly, any design modifications observed to be needed on the TV8117 rotor to accommodate the ceramic rotor would be implemented on the modified tool.

Actual ceramic rotor fabrication began in August, 1985. The existing TV8177 tooling was used to produce wax injection patterns. Plaster bases used initially produced a rotor with a 1 5/8-inch-diameter shaft.

The material system used to cast the initial rotors was based on the Code 1 and Code 2 formulations. The majority of the rotors cast used Code 2/GTE SN-502 formulation.

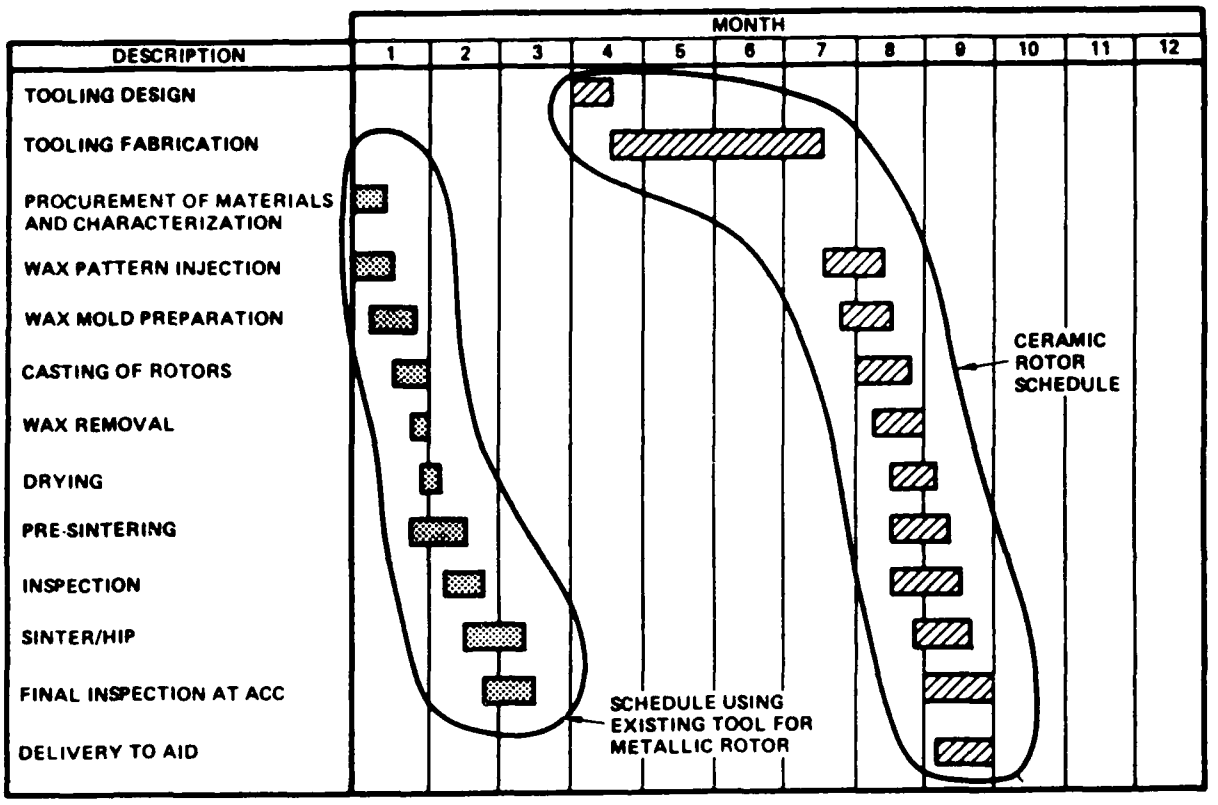

Figure 5-25. ACC Program Schedule

Figure 5-26. TV8117 Injection Wax Pattern (Left), TV8117 Wax Shell/Plaster Assembly (Right)

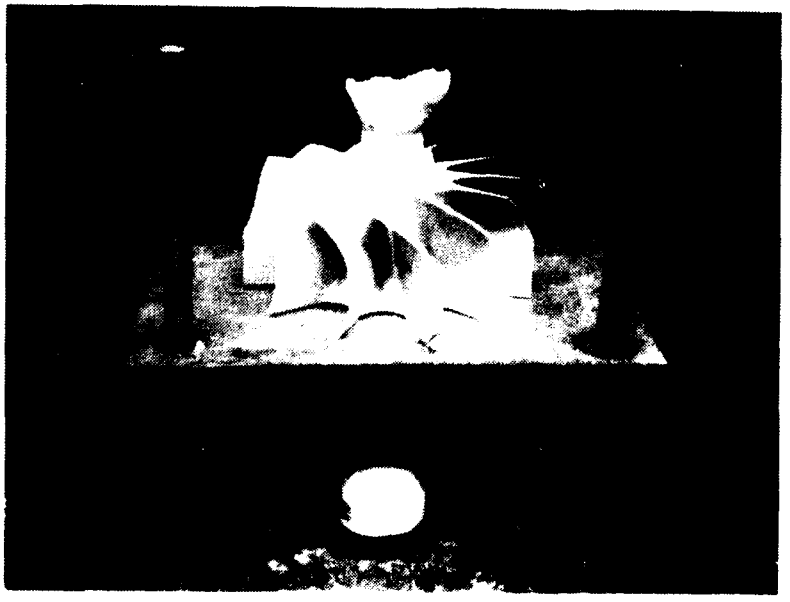

Figure 5-27. Ceramic TV8117 Rotor Used for Density and Shrinkage Measurements

Twenty rotors were cast using the TV8117 rotor with the 1 5/8-inch-diameter shaft. All of the rotors cast were found to have defects. Several rotors were suitable to be used to make density and shrinkage measurements (Figure 5-27). Based upon the results from the 20 rotors cast, Code 2/GTE SN-502 and Code 27 rotors were continued; rotors using Code 1 and 2/Starck H-2 and Code 1/GTE SN-502 were discontinued. Shrinkage factors for the Code 2 and Code 27 rotors were found to be the same and were incorporated into the modified tooling design.

5.3.2. Phase Two (Modified Metal Blade Tooling). During the initial casting of the ceramic rotors in Phase Two, a decision was made to reduce the shaft diameter from 1 5/8 inch to 7/8 inch (see Figure 5-28). The justification for reducing the shaft diameter was to reduce the amount of machining stock on the rotor shaft and produce a part closer to net-shape. During experimental casting of the smaller diameter shaft rotor, final consideration was made to design the modified plaster tooling with a smaller diameter shaft (1 5/8 inch to approximately 1 inch). While the modified tooling was being built, continued casting studies were carried out using the existing TV8117 tooling.

Twenty rotors were cast using the TV8117 configuration with a 7/8-inch-diameter shaft. Both Code 2 and Code 27 material systems were used in casting rotors. No rotors were qualified as acceptable. The majority of defects were blade cracking or incomplete blade casting (entrapped air/residual soluble wax) (see Figure 5-29). One rotor was processed through sinter-HIP with no casting related defects. However, blade warpage was apparent after the rotor was sinter-HIP'ped. Several rotors showing defects were also sinter-HIP'ped to verify process parameters during sinter-HIP. From the difficulties observed with the Code 27 rotors, work on the Code 27 rotors was phased out. Many rotors using the Code 2/GTE were rejected early in processing due to a shipment of GTE SN-502 silicon nitride which produced a poor quality slip and eventually an unsatisfactory green rotor. Because of the problems with GTE silicon nitride, H.C. Starck H-2 in a Code 2 formulation was re-introduced and wheels were cast. Despite the problems with consistency from using GTE silicon nitride, rotors using GTE still showed the best potential to be acceptable.

Up to this point, actual yield for the ceramic rotor was non-existent. However, consideration had to be made for the fact that ceramic rotor fabrication was being attempted with tooling not initially designed for ceramic fabrication. Based upon the potential of correcting previous defects with the modified tooling, meeting the original schedule was still feasible, even after accounting for the time needed to produce rotors at a lower yield rate of 30 percent.

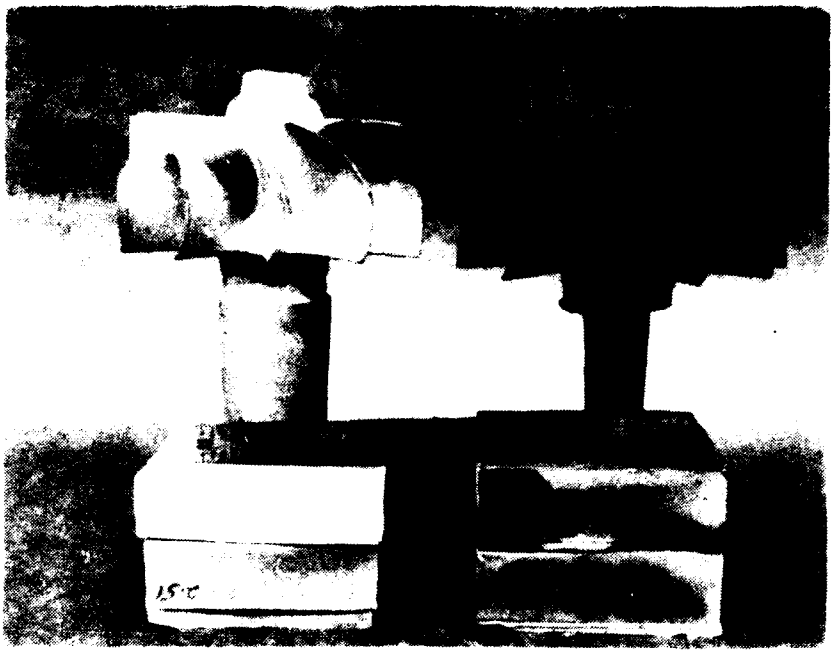

Figure 5-28. TACOM Ceramic Rotor with 1 5/8-inch-diameter Shaft (Left), TACOM Ceramic Rotor with 7/8-inch diameter Shaft (Right)

Figure 5-29. TACOM Rotor Showing Blade Cracking (TV8117 Design)

5.3.3. Phase Three (Ceramic Rotor Tooling). In Phase Three, the Code 2/GTE SN-502 Si_3N_4 formulation was selected to slip cast rotors using the modified tooling. The modified wax injection die was received March 24, 1986. Additional wax and plaster tooling was received April 1, 1986. Included in tooling received was: 1) An injected wax pattern fixture to coat the injected wax pattern with nonsoluble wax and machine the wax pattern to proper dimensions for alignment; 2) A plaster mold die designed to align the wax shell to the plaster and to produce a tapered shaft that allows for easier removal of the rotor from the plaster; 3) A wax pattern alignment fixture to affix the wax pattern shell to the plaster. The modified rotor was designed with more gradual transition points (especially shaft/rotor transition) and dimensionally larger blades to help alleviate defects during casting.

The first two rotors using the updated tooling were able to be processed through sinter-HIP with defects only becoming apparent after sinter-HIP'ping. Normally, several casting attempts are necessary to eliminate major defects and establish a casting procedure. To be able to process the initial castings up to sinter-HIP without apparent defects was encouraging. However, adjustments made in casting procedures to eliminate remaining defects were not successful. In some cases, more defects developed in the rotor at earlier stages of rotor processing.

Seventy rotors were processed using the new tooling as designed. No rotors were fabricated that would be classified as acceptable. Several rotors having defects were processed and evaluated. All rotors cast used the GTE SN-502/Code 2 silicon nitride formulation. The majority of defects that showed consistently were blade cracking, blade voids (due to air entrapment or residual soluble wax in the casting shell), cracks at the rotor/nose transition and poor surface finish. (see Figures 5-30 through 5-32).

5.3.4. Phase Four (Alternate Process). A major re-evaluation of casting procedures, added at no cost to the Government, was performed. With all previous castings, the TACOM rotors were cast in a closed-blade configuration; the blades themselves were not directly exposed to a plaster casting surface. The reasoning for the closed-blade configuration was economics. By using the closed-blade method of casting, a part closer to net-shape could be produced, substantially reducing any machining of the rotor at the blade areas. By reducing rotor machining, the rotor could be produced at a significantly lower cost. However, with the lack of success using the closed-blade method of casting, other casting procedures were in order.

Several modifications were attempted to produce an acceptable rotor. One attempt was to modify the plaster by enlarging the shaft diameter to increase the casting surface of the rotor. The major modification effort, however, was placed on opening the backface of the wax shell and expose the blades to the plaster base, similar to the AGT-101 casting procedure. The advantages of an open bladed modified casting were a more uniform casting

Figure 5-30. TACOM Rotor Showing Extensive Blade Defects

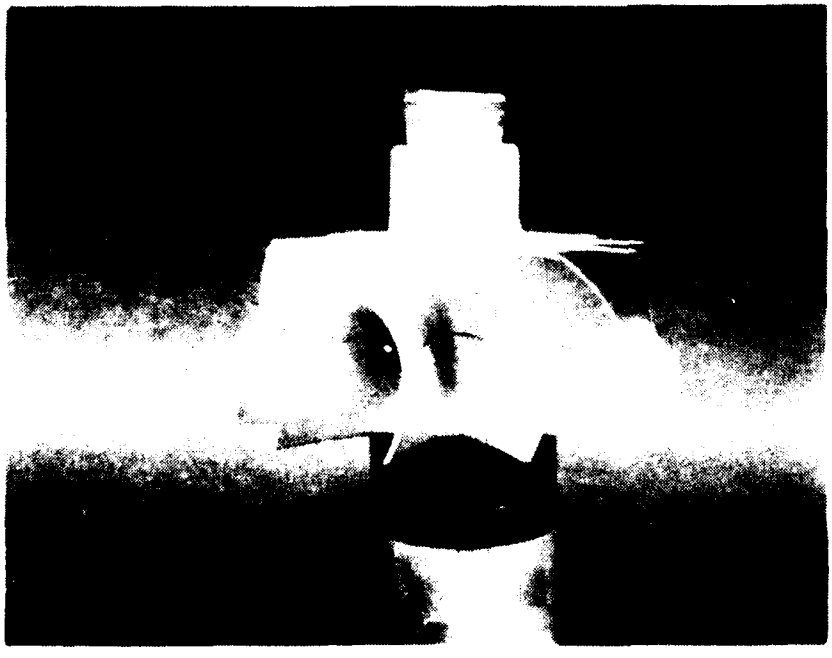

Figure 5-31. TACOM Rotor with Cracking in Blade Transition Areas

Figure 5-32. TACOM Rotor Showing Incomplete Casting at Nose

(especially in the blades) in a shorter casting time. However, significant machining is necessary on the backface and blades to bring the rotor into dimensional acceptance. In addition, extensive modifications were needed on the wax shell and plaster base to maintain reasonable dimensional integrity. A problem that arose due to the plaster die modification in the open-bladed casting was increased difficulty in removing the rotor from the plaster base. Several rotors were broken due to difficulties in removing the rotor from the plaster.

Open-bladed castings showed better results in terms of blade integrity. However, blade improvements were offset by previously mentioned difficulties in removing the rotor from the plaster molds. Those rotors able to be processed showed cracking in presintering. Several rotors that were acceptable through presintering were sinter-HIP'ped. However, the sinter-HIP furnace malfunctioned resulting in cracking of the rotors. Two additional rotors were presintered and awaiting sinter-HIP when it became clear that due to time and funding constraints, the substantial development effort still needed was not realistsically within the current contract.

5.3.5. Analysis/Summary. As described, the casting method used on the TACOM rotors can be referred to as a close-blade casting system: the rotor blades are not directly exposed to a casting surface. An AGT-101 rotor is produced using an open-blade system of casting: the rotor blades are directly exposed to a casting surface (Figure 5-33). Advantages of open-blade casting are more uniform casting of the rotor blades and having the blades cast at the same rate as the rest of the rotor. The major disadvantage of open-blade casting is the amount of excess material (machine stock) on the rotor blades that requires extensive machining.

When discussions were held to decide upon final fabrication criteria for the TACOM rotor, the AGT-101 method of casting was considered. Because of the additional machining (and cost) to bring a rotor to dimensional specification, open-blade casting was not considered acceptable for the TACOM rotor, and the closed-blade casting system was selected. The closed-blade method would produce a rotor closer to net shape. The impact of selecting the closed-blade system versus the open-blade system in terms of casting parameters were considered at the time as acceptable trade-off for its cost reduction potential.

By using the closed-blade casting system, the rate of casting is slowed and the uniformity of casting is restricted. For example, a TACOM rotor casting in the closed-blade system would cast initially at the rotor shaft area since the rotor is directly exposed to plaster. The rotor would slowly cast away from the shaft area to the blade/hub transition and the lower blade area at the same time while casting by evaporation is taking place at the nose area. The

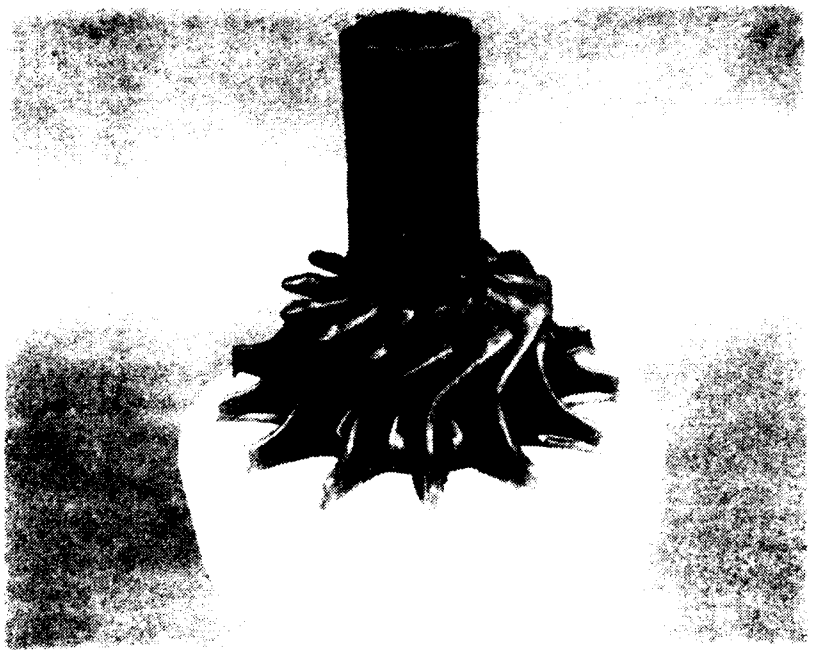

Figure 5-33. AGT-101 Mold Assembly

last area to cast is the upper portion of the blades. The majority of the defects seen in the TACOM rotors were in this region due to uncast slip or cracking that developed in the blades. Despite repeated modifications, the closed-blade system did not allow for a uniform casting.

In comparison, the open-blade system exposes the blade edges to a plaster surface. The blades (and the entire rotor) cast at a more uniform and accelerated rate (1/2 the casting time of close-bladed casting). Since the rotor is exposed to more plaster, however, the rotor is more prone to cracking due to overcasting. In the limited amount of open-blade casting with the TACOM rotor, overcasting was shown to be a problem. In addition, the improvised modifications made to fabricate a rotor in the open-blade style resulted in rotor removal problems from the plaster. However, overall blade integrity was better than the rotors cast in the closed-blade system.

5.4. Ceramic Rotor Fabrication - Alternate Ceramic Source

5.4.1. Introduction. In order to fulfill the hardware deliverable requirements of the TACOM Program, Garrett explored other potential ceramic suppliers with the intent of purchasing ceramic hardware only and not to subcontract for development of a ceramic process.

Garrett has been actively working with a number of ceramic suppliers to develop ceramic turbocharger rotors for passenger cars and commercial diesel applications. These rotors ranged in rotor diameters from 48 mm to 76 mm. The three principal suppliers were Japanese sources: Kyocera, NGK Insulator and NTK Ceramics Company (NGK Sparkplugs). All three suppliers have excellent processing capability, very good material and excellent research and development facilities devoted to producing structural ceramic materials and processes.

Most significantly, the United States-based suppliers are the furthest behind in the development of process capability. GTE, Norton/TRW, Carborundum have all experienced the same problem as ACC and to date are unable to produce satisfactory ceramic rotors for turbochargers.

Although all of the three Japanese suppliers have demonstrated net-shape capabilities, Kyocera was selected because of the following: 1) Utilizes the same open-blade slip-casting process; 2) Consistently provides the best material properties and Weibull distribution; and 3) Demonstrated the ability to provide castings quickly.

The following discussions regarding Kyocera ceramic rotor design are excerpts from Reference 1.

5.4.2. Ceramic Rotor Design. Because of their brittle nature, ceramics can be abruptly fractured when subjected to excessive stress. While metals deform under similar conditions, ceramics are limited by this relatively low fracture resistance. Consequently, small defects inside a ceramic component or on its surface are very undesirable for high-stress components. Metals have, therefore, traditionally been considered more attractive for these applications.

Recently, however, the mechanical characteristics and structural reliability of ceramic materials have been significantly improved. The intrinsic bond strength of silicon nitride has been increased substantially and maintained at higher temperatures. The size and number of strength-limiting defects diminish with every additional processing experience and each refinement in processing.

Today, the relationship between the strength of test specimens and strength, life and failure probability of actual ceramic components can be formulated by fracture mechanics and Weibull statistics. Figure 5-34 shows the Weibull distribution of the fracture stress of silicon nitride test specimens which were dry pressed and sintered in the shape of small bars as well as specimens which were cut from turbine wheel hubs made by slip casting and sintering the same material.

Table 5-1 shows the material properties of the Kyocera silicon nitride SN220M which has been selected for this application because of its fracture toughness, thermal shock resistance and process capability.

5.4.3. Ceramic Turbine Wheel Production. In order to produce ceramic turbine wheels commercially, every step of the production process must be well controlled and performed with skilled hands. Among many processes beginning from raw material synthesis to final inspection, the shape-forming process has the strongest influence on production cost. Near-net shape forming such as injection molding and slip casting are needed to produce such complex-shaped ceramic components such as turbine wheels.

In injection molding, ceramic powders are blended with organic binders, (thermoplastic resins and plasticizers) of almost equal volume at elevated temperatures and forced to flow through an orifice into the cavity of a preheated tool. After the binder is burned out, the ceramic is sintered to near-net shape.

In slip-casting, a slurry of uniformly dispersed ceramic powder mixture is cast into plaster molds. Liquidity and viscosity can be lowered through the selection of organic additives such as binders, wetting agents and deflocculents. Uniform and dense particle packing without particle agglomeration is achieved in carefully made slurries. The slip-casting process provides a process for

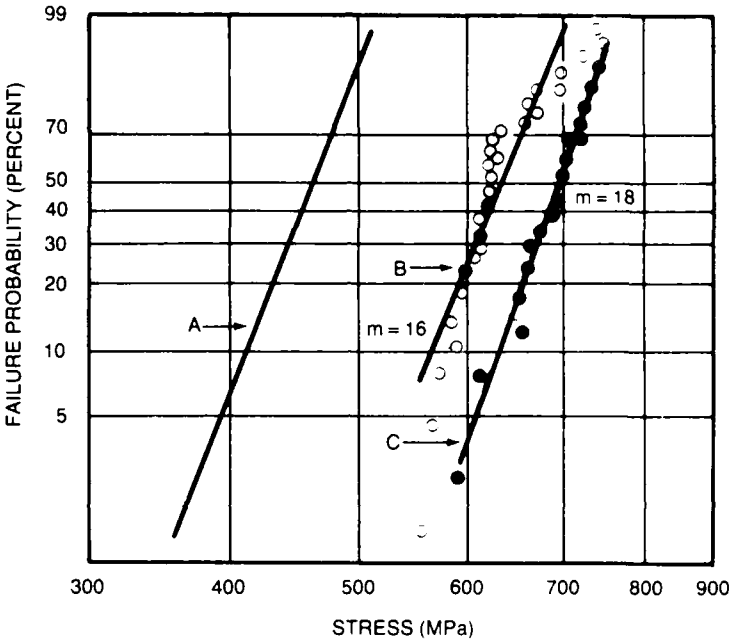

Figure 5-34. Failure Probabilities of Silicon Nitride (Kyocera SN 220M)

producing defect free rotors because of higher casting fluidity and lower amounts of binders. Because of uniform and dense particle packing, higher green density, and lower firing shrinkage, fired wheels have uniform mechanical properties and good dimensional accuracy. Careful fabrication of plaster molds minimizes machining after firing.

Figure 5-35 shows the process flow for ceramic rotor casting and shaft wheel assemblies.

5.4.4. Non-Destructive Evaluation. To insure the reliability of ceramic turbine wheels on the basis of fracture mechanics and Weibull statistics, it is important to maintain the mechanical properties of the ceramic material. The mechanical properties of ceramics are extremely sensitive to defects which have been introduced accidently during processing. Major causes of defects are as follows:

- Nonhomogeneity in casting slurry
- Pores in slurry
- Nonhomogeneity in drying shrinkage and firing shrinkage
- Flaws and chips in machining and handling
- Nonuniform distribution of the braze material

The number of defects could be minimized by careful process control, but it is virtually impossible to eliminate all of the defects from production rotors. It is, therefore, important to detect all of the strength-limiting defects nondestructively and remove the defective parts from the process.

The maximum allowable size (Amax) of defects can be calculated from the following relationship:

$$K1C = Y * Smax \sqrt{Amax}$$

Where K1C is the critical stress intensity factor of the fracture toughness of the material and Smax is the maximum stress.

For example, in the case of a 56 mm diameter wheel with a maximum design speed of 170,000 r/min, Smax is equal to 240 MPa at 120 percent overspeed. By substituting K1C with a value of 7.4 shown on Table 5-1, Amax is calculated to be 180 μm. TV81 maximum stress is 24,000 psi (166 MPa).

Defects larger than 180 μm can be detected by existing NDE methods. Table 5-2 shows the basic NDE methods for various types of defects.

5.4.4. Quality Assurance. The quality assurance procedure used by Kyocera to maintain strict process control is shown on Table 5-3. The chart identified the process flow chart, process name, control point, method for check, sample lot and remarks.

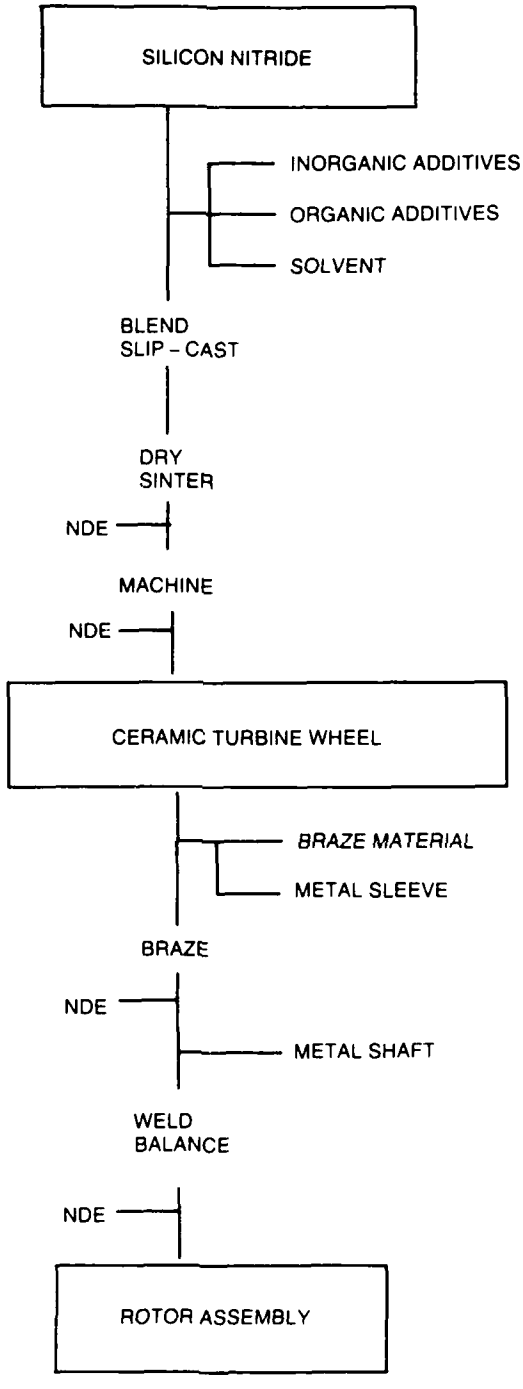

Figure 5-35. Process Flow Diagram for Ceramic Turbine Wheels and Rotor Assemblies

Table 5-1. Material Properties of SN220M

BULK DENSITY	3.19 (3.16)
FLEXURAL STRENGTH *	
RT	679MPa (627MPa)
800°C	679MPa
1000°C	598MPa
1200°C	390MPa
YOUNG'S MODULUS	293GPa
POISSON'S RATIO	0.28
HARDNESS HRa	92.0
TOUGHNESS K1c**	7.4MN/$m^{3/2}$(7.3MN/$m^{3/2}$)
COEFFICIENT OF LINEAR THERMAL EXPANSION (40~900°C)	3.1 × 10^{-6}/°C
THERMAL CONDUCTIVITY	25W/mK

( ): THE PROPERTIES OF SPECIMENS CUT FROM SLIP-CAST ROTORS

*4 – POINT BENDING (CROSS SECTION: 3 × 4, INNER SPAN: 10, OUTER SPAN: 30mm)

**INDENTATION METHOD

Table 5-2. NDE Methods for Various Types of Defects

NDE TIMING	TYPE OF DEFECTS	NDE METHOD
AFTER SINTERING	SURFACE CRACK	FLUORESCENT DYE PENETRANT
	INSIDE CRACK	ULTRASONIC
	INSIDE VOID	X – RAY RADIOGRAPHY
AFTER MACHINING	CHIP	VISUAL
	MACHINING FLAW	FLUORESCENT DYE PENETRANT
AFTER BRAZING	BRAZE STAGNANCY	ULTRASONIC C – SCAN
BEFORE SHIPPING	CHIP	VISUAL
	CRACK	VISUAL

Table 5-3. Quality Assurance Table for Standard Process (1/2)

ARTICLE (CERAMIC ROTOR)	CUSTOMER GARRETT CORPORATION	CUSTOMER'S PART NO. T-3, T-4, T-25, TV-81	DOCUMENT NO. KT-10802-006

DATE FEBRUARY 27, 1987	GENERAL MANAGER APPROVED	DEVELOP-MENT CHECKED	QUALITY ASSURANCE		MANUFACTURING	
KYOCERA CORPORATION CORPORATE FINE CERAMICS DIV AUTOMOTIVE COMPONENTS DEP (KAGOSHIMA KOKUBU PLANT)			CHECKED	ARRANGED	CHECKED	ARRANGED

PROCESS CHART		PROCESS NAME	CONTROL POINT	METHOD FOR CHECK	SAMPLE	REMARKS
△	1	RAW MATERIAL				
◇	2	ACCEPTANCE	PURITY	MAKER'S INSPECTION	EVERY LOT	400 kg/L
			IMPURITIES (Fe. Al. Ca)			
		INSPECTION	GRAIN SIZE	PRETESTING	1/LOT	
			STRENGTH	(TP FROM ACTUAL ARTICLE)		
○	3	PREPARING	POWDER COMPOSITION	STEELYARD	EVERY LOT	
			SOLVENT COMPOSITION	ELECTRONIC BALANCE	EVERY LOT	
			SLIP COMPOSITION	ELECTRONIC BALANCE	EVERY LOT	
			SLIP VISCOSITY	E-TYPE VISCOMETER	EVERY LOT	
			FORMING RATE	GAUGE	EVERY LOT	
○	4	CASTING	MOLD MATERIAL	MAKER'S INSPECTION	EVERY LOT	PRODUCT'
			MOLD POROSITY	MERCURY METHOD	1/LOT	LOT
			MOLD WEIGHT	ELECTRONIC BALANCE	1/LOT	START
			MOLD LIFE SPAN	CHECK SHEET	EVERY LOT	
			MOLD CHIP	VISUAL INSPECTION	EVERY LOT	
			MOLD SURFACE	VISUAL INSPECTION (BOUNDARY SAMPLE)	EVERY LOT	
			SLIP FLOW RATE	FLOW RATE METER	1/DAY	
			MOLDING PRESSURE	PRESSURE GAUGE	100%	
			MOLDING TIME	TIMER	100%	
○	5	MOLD REMOVING				
			CASTED OUTLOOK	VISUAL INSPECTION (BOUNDARY SAMPLE)	100%	
			SERIAL NUMBER (IN-HOUSE)	VISUAL CHECK	100%	
○	6	DRYING	DRYING TEMPERATURE	THERMOMETER	1/CHARGE	DRIER
			DRYING TIME	WATCH	1/CHARGE	
○	7	DEWAXING	DRYING TEMPERATURE 1	ATTACHED THERMOMETER	1/CHARGE	
			DRYING TEMPERATURE 2	ATTACHED THERMOMETER	1/CHARGE	
			DEWAXING TEMPERATURE	THERMOCOUPLE	1/CHARGE	
			CONVEYING SPEED	STOPWATCH	1/CHARGE	
			N GAS FLOW RATE	FLOW METER	1/CHARGE	
			FOMING GAS FLOW RATE	FLOW METER	1/CHARGE	
○	8	BISQUE MACHINING	BISQUE OUTLOOK	VISUAL INSPECTION (BOUNDARY SAMPLE)	100%	
			BISQUE SIZE	CALIPER	1/20	
○	9	FIRING	FIRING CONDITION	THERMOCOUPLE	EVERY LOT	
			SHRINKAGE	CALIPER	1/LOT	
			FLEXURAL STRENGTH	JIS-4 POINT FLEXURAL METHOD (JIS R1601)	2/LOT	

Table 5-3. Quality Assurance Table for Standard Process (2/2)

PROCESS CHART	PROCESS NAME	CONTROL POINT	METHOD FOR CHECK	SAMPLE	REMARKS
◇ 10	FIRING	FIRED WARE OUTLOOK	FLUORESCENT PENETRANT INSPECTION	100%	
	INSPECTION	INSIDE CRACK	ULTRASONIC INSPECTION	100%	
		INSIDE PORE	X-RAY INSPECTION	100%	
○ 11	M.C.ROUGH GRINDING				
○ 12	MASS	INITIAL UNBALANCE	BALANCER MACHINE	100%	
	CENTERING	MENDED UNBALANCE	DIAL GAUGE	100%	
		CENTER HOLE SHAPE	TRILEAD TETRAOXIDE (BOUNDARY SAMPLE)	100%	
○ 13	FINAL	NOSE OD	MICROMETER	100%	
	GRINDING	BLADE OD	CALIPER	100%	
		SHAFT HUB OD	MICROMETER	100%	
		GROOVE POSITION	PROJECTOR	100%	
		BACKFACE SHAPE	INK CHECK	100%	
		SHROUD LINE	PROJECTOR	1/LOT	
○ 14	BOSS CUTTING	BOSS LENGTH	GAUGE	100%	
◇ 15	UNBALANCE INSPECTION	RESIDUAL UNBALANCE	BALANCER MACHINE	100%	
◇ 16	FINAL	FINAL OUTLOOK	FLUORESCENT PENTRANT INSPECTION	100%	
	INSPECTION	INSIDE CRACK	ULTRASONIC	100%	
		LOT NUMBER	VISUAL CHECK	100%	
▽ 17	SHIPPING	PACKAGE OUTLOOK	VISUAL CHECK	100%	
◇ 18	ENVIRONMENT	COLLISION-PROOF	SPIN TEST	INITIAL	
	TEST	HEATSHOCK-PROOF	QUENTING IN WATER	2/YEAR	

5.5. Report of Test Results

5.5.1. Test Matrix. The following list summarizes the number of components and turbocharger assemblies which were tested under the various conditions described in this report. A parts list for the basic unit is contained in Appendix A.

Test	Test Hardware	Serial Number
Static Test	40 test bars cut from 5 ceramic rotors	-
Hot Spin Test	3 ceramic rotor turbochargers*	TAC 001 TAC 002 TAC 003
Aero Performance	One ceramic rotor turbocharger One metal rotor turbocharger	TAC 007 TAC 009
Shaft Motion	One ceramic rotor turbocharger with special compressor nut and modified compressor housing for two shaft motion probes	TAC 008
Durability	4 ceramic rotor turbochargers	TAC 004 TAC 005 TAC 006 TAC 008

*These units to be delivered to TACOM along with two new ceramic rotor/shaft assemblies and 15 ceramic rotors.

5.5.2. Hot Spin Tests. To demonstrate the integrity of the three turbochargers shipped to TACOM, each unit was installed on a gas stand and operated at a speed of 80,000 r/min for 10 minutes at 649 C turbine inlet temperature.

The laboratory test log sheets for each unit (serial numbers TAC 001, 002 and 003) as well as the assembled dimensions of the units are included in Appendix B.

Each unit successfully completed the test.

5.5.3. Aerodynamic Performance. The objective of these tests was to document the performance of the ceramic turbine wheel and compare it with the existing metallic design.

Turbine flow and efficiency characteristics were determined as a function of pressure ratio and rotational speed in accordance with standard procedure TI056. Both ceramic and metallic wheels were tested to provide back-to-back performance comparisons.

See TI056 in Appendix C.

Turbine aerodynamic performances were measured in the Garrett Laboratory in accordance with the Garrett Standard TI056 test procedure. In the first test series, a ceramic wheel unit (S/N TAC 007) and a metal wheel unit (S/N TAC 009) were tested in the same turbine housing. Figure 5-36 shows a Garrett turbocharger test cell with a turbocharger of similar size to the TV81 (but not the actual TACOM unit).

The results of the first test series are shown in Figures 5-37 and 5-38. The flow capacity of both metal and ceramic wheels are the same, but the efficiency of the ceramic wheel is down one point at mid-pressure ratios and down three points at high-pressure ratios.

While the ceramic wheel design (blade shapes) were based on the metal wheel design, certain requirements for ceramic wheels cause the two wheels to be slightly different. These differences were reviewed to determine which factors were causing the performance loss.

1. The ceramic wheel blade tips are about 40 percent (.065 vs. .045 inches) thicker than the metal wheel blade tips. See Figure 5-39.

2. The metal wheel has slightly more blade "wrap" than the ceramic wheel. See Figure 5-40. This occurred because the ceramic wheel exducer has a slight cut-back to reduce blade root stress.

3. At operating temperature, the wheel-to-housing clearance differs between the two types of wheels because of the different thermal expansion properties of the two materials. The calculated change in wheel-to-housing clearances from cold to hot (482 C gas stand turbine inlet temperature) is .004 inches radial and .002 inches axial greater for the metal wheel and .0115 inches radial and .004 inches axial greater for the ceramic wheel.

4. The ceramic blade surfaces are slightly rough because of the slip-casting manufacturing method.

Of the factors which may be causing the performance difference in the ceramic wheel unit, the wheel-to-housing clearance can be readily evaluated. A second series of tests on the performance gas stands was run to measure the effect of wheel-to-housing clearance. A turbine housing was modified to obtain the reduced clearances of .021 inches radial and .023 inches axial (compared to standard metal wheel clearances of the metal wheel test unit of .031 inches radial and .025 inches axial). All parts of the

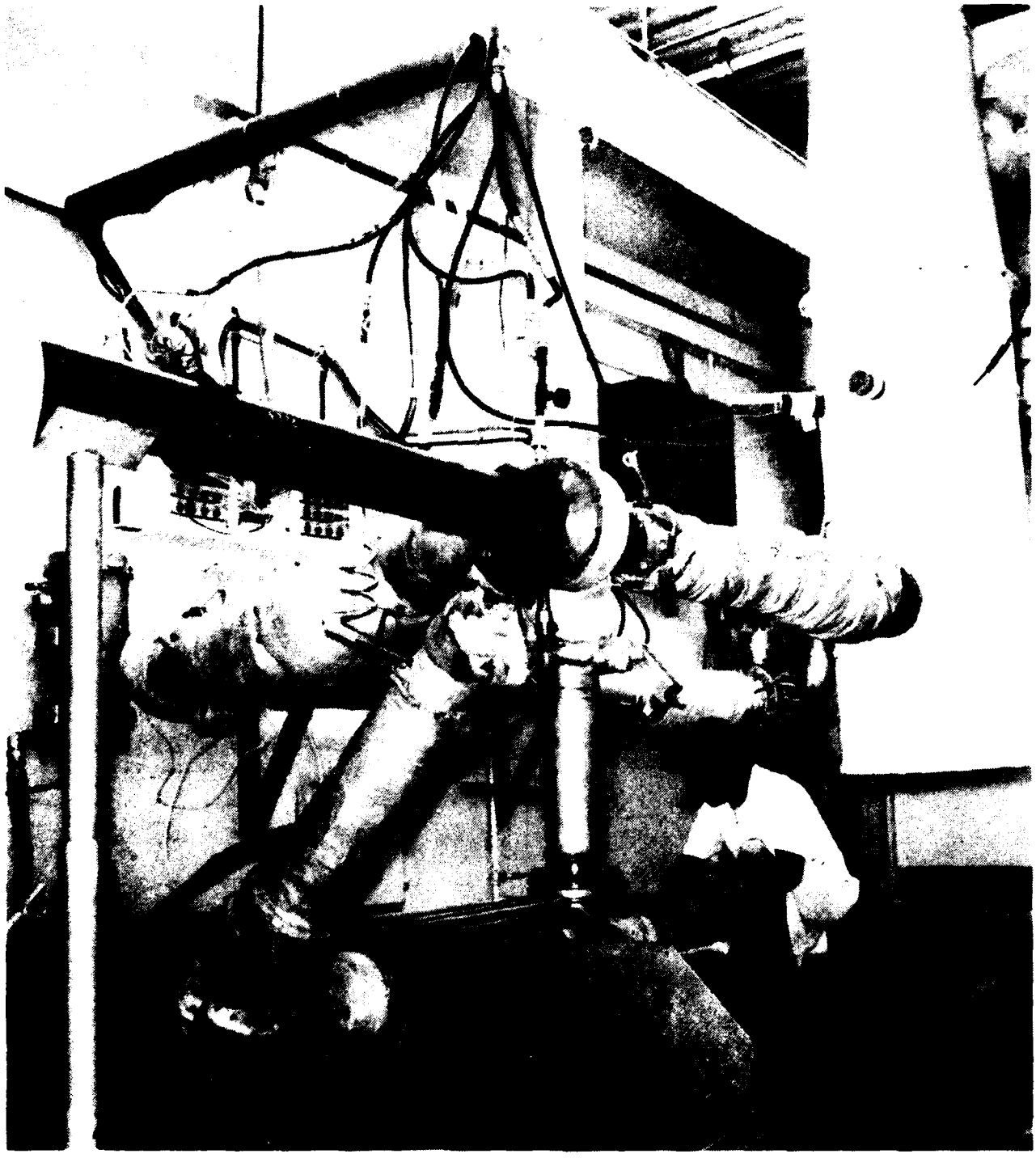

Figure 5-36. Turbocharger Test Setup

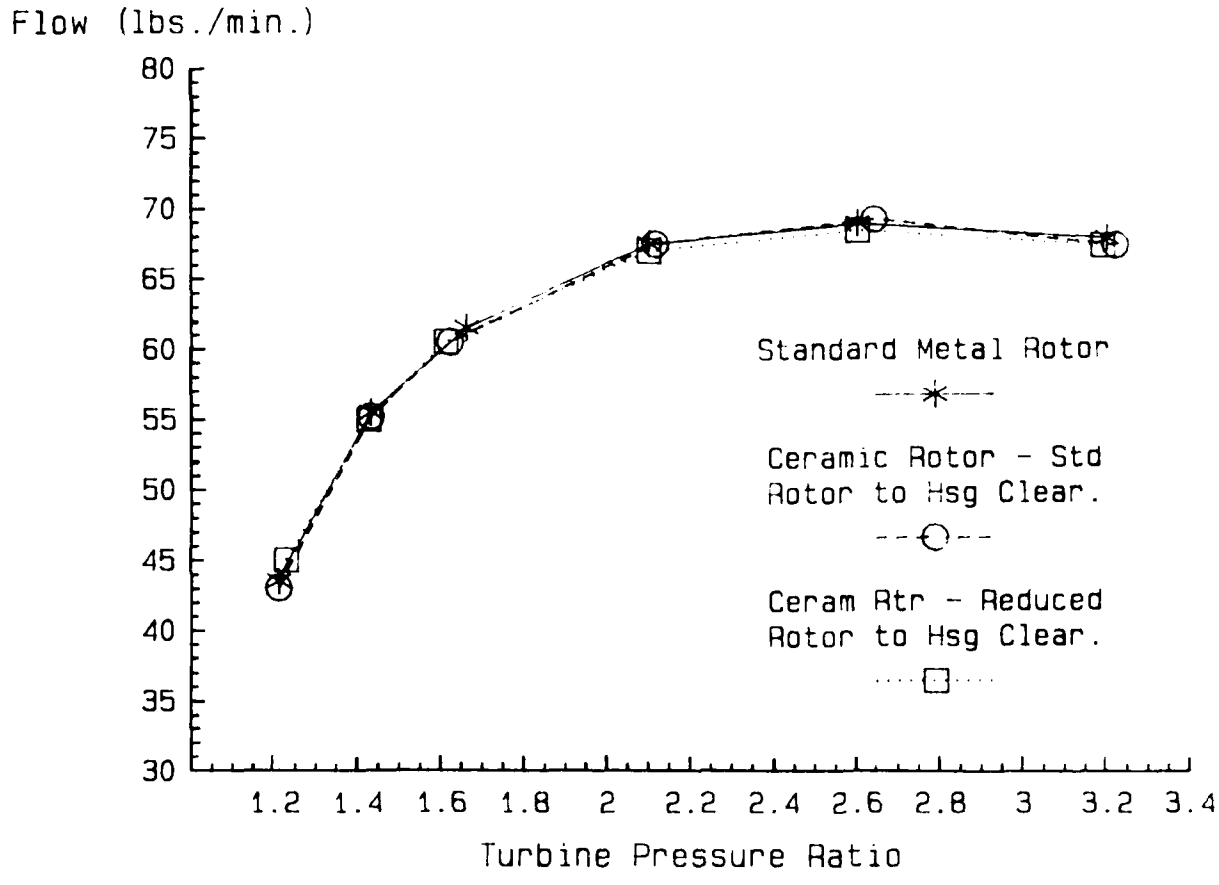

Figure 5-37. TACOM-TV81 Ceramic vs. Metal Rotor Turbine Performance

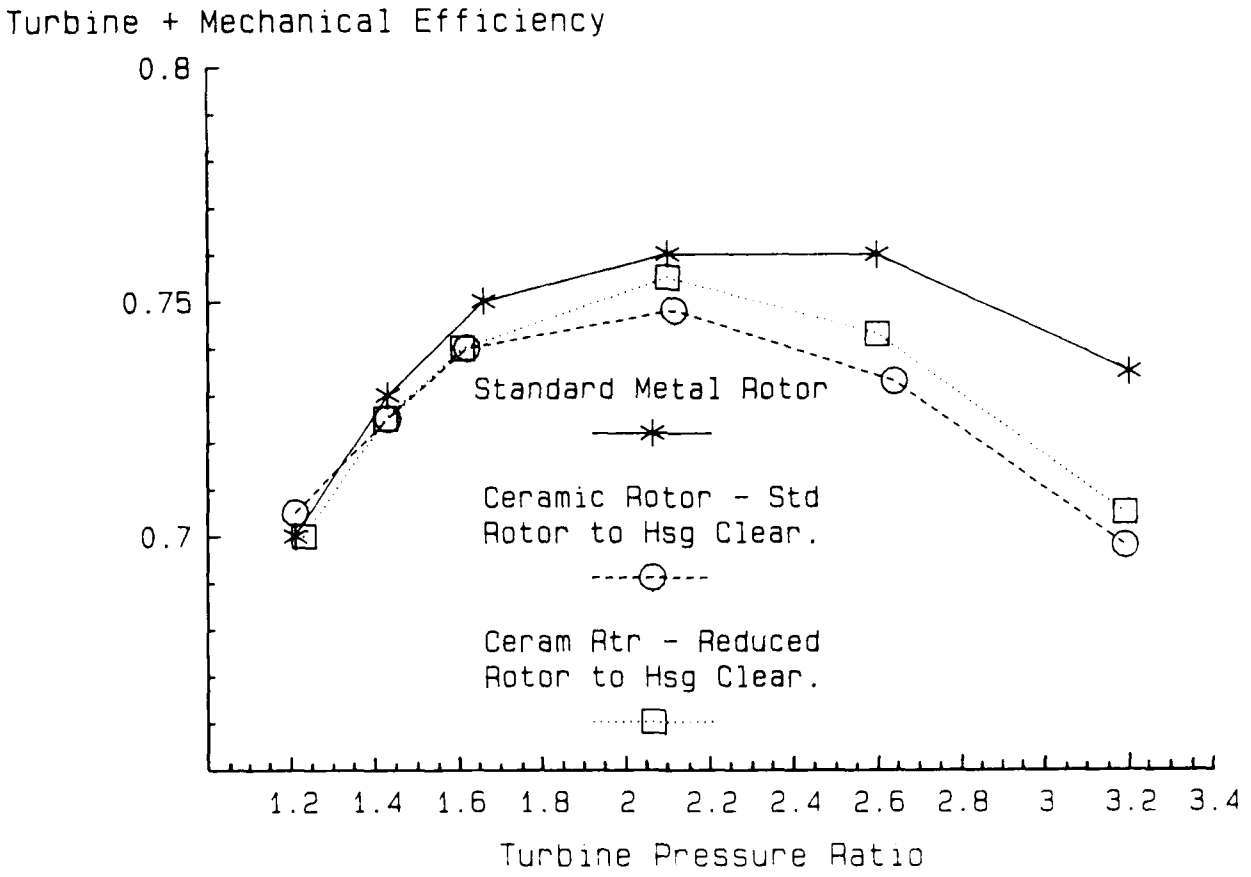

Figure 5-38. TACOM-TV81 Ceramic vs. Metal Rotor Turbine Performance

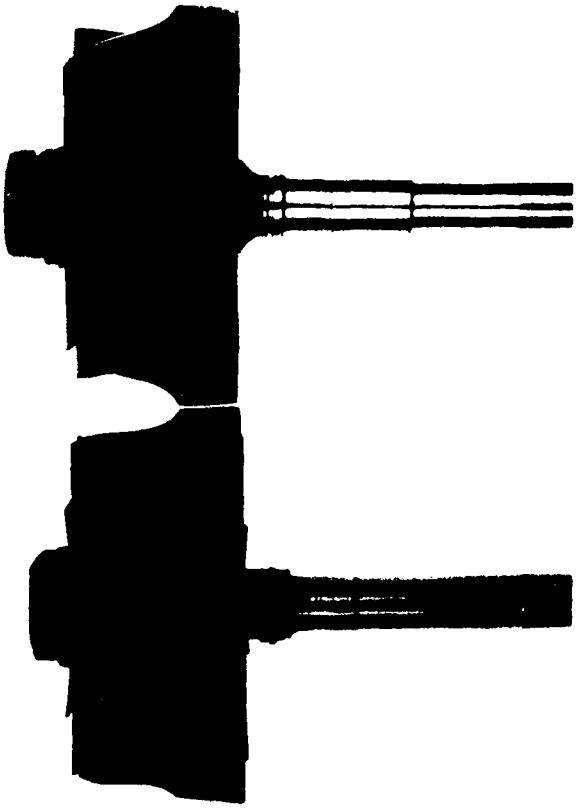

Figure 5-39. Comparison of Wheel Blade Tip Thickness, Ceramic Rotor at Top of Photograph, Metal Rotor at Bottom

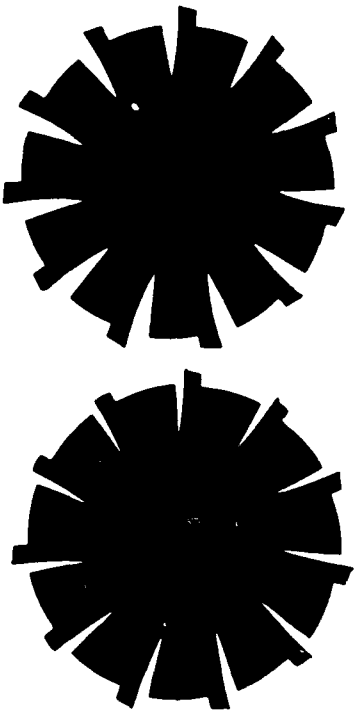

Figure 5-40. Comparison of Blade "Wrap" Ceramic Rotor at Top of Photograph, Metal Rotor at Bottom

reduced clearance ceramic wheel unit were the same as in the first test except the housing. The results of this performance test are shown in Figures 5-37 and 5-38. Compared to the earlier ceramic wheel test with standard clearances (Test No. I.E. 380) the reduced clearances improved turbine efficiency by about one point at high pressure ratios and was the same at low- and mid-pressure ratios.

The metal wheel unit was retested (partial test, three speedlines) during this second series to check on test stand repeatability. The results were essentially identical with the first test. (Compare Map Test No., I.E. 542 and I.E. 379 in Appendix C. Also in Appendix C are maps of the ceramic wheel tests and certain critical assembly measurements.)

The conclusions drawn from these tests are that the ceramic wheel, while having exactly the same flow capacity as the metal wheel, is slightly less efficient. But, by reducing the wheel clearances, which is allowable because of the ceramics low coefficient of thermal expansion, the efficiency difference is, for practical purposes, of minor significance. Based on the experience learned from this design and these tests, future ceramic wheel designs should consider improving the blade surface finish, along with reduced wheel clearance.

5.5.4. Shaft Motion. The objective of these tests was to establish that the turbocharger rotating assembly does not exhibit unstable behavior within the normal operating speed range due to the changes in weight/inertia of the wheel and differences in shaft stiffness associated with the change from a metallic to ceramic wheel casting.

Shaft motion characteristics are determined by measuring the dynamic excursions of the rotating assembly outboard of the compressor wheel. Proximity probes located 90 apart provide X-Y shaft position data and with appropriate readout instrumentation, the output can be formatted to show orbital characteristics, spectral frequency analysis and total excursion as a function of rotational speed. The initial tests were scans across the operational speed range to establish worst-case conditions. Orbital and frequency analyses were made at conditions where peaks, spikes or other unusual conditions were revealed by the speed sweeps.

The complete test procedure is explained in Appendix D.

For the shaft motion test, one unit (S/N TAC 008) was randomly selected from the group of test and shipping units. Certain critical measurements made on this unit are listed in the Appendix. The bearing clearances are graphically shown in relation to the total tolerance range of clearances on Figure 5-41. The bearing clearances of this unit are close to mean value clearances. The

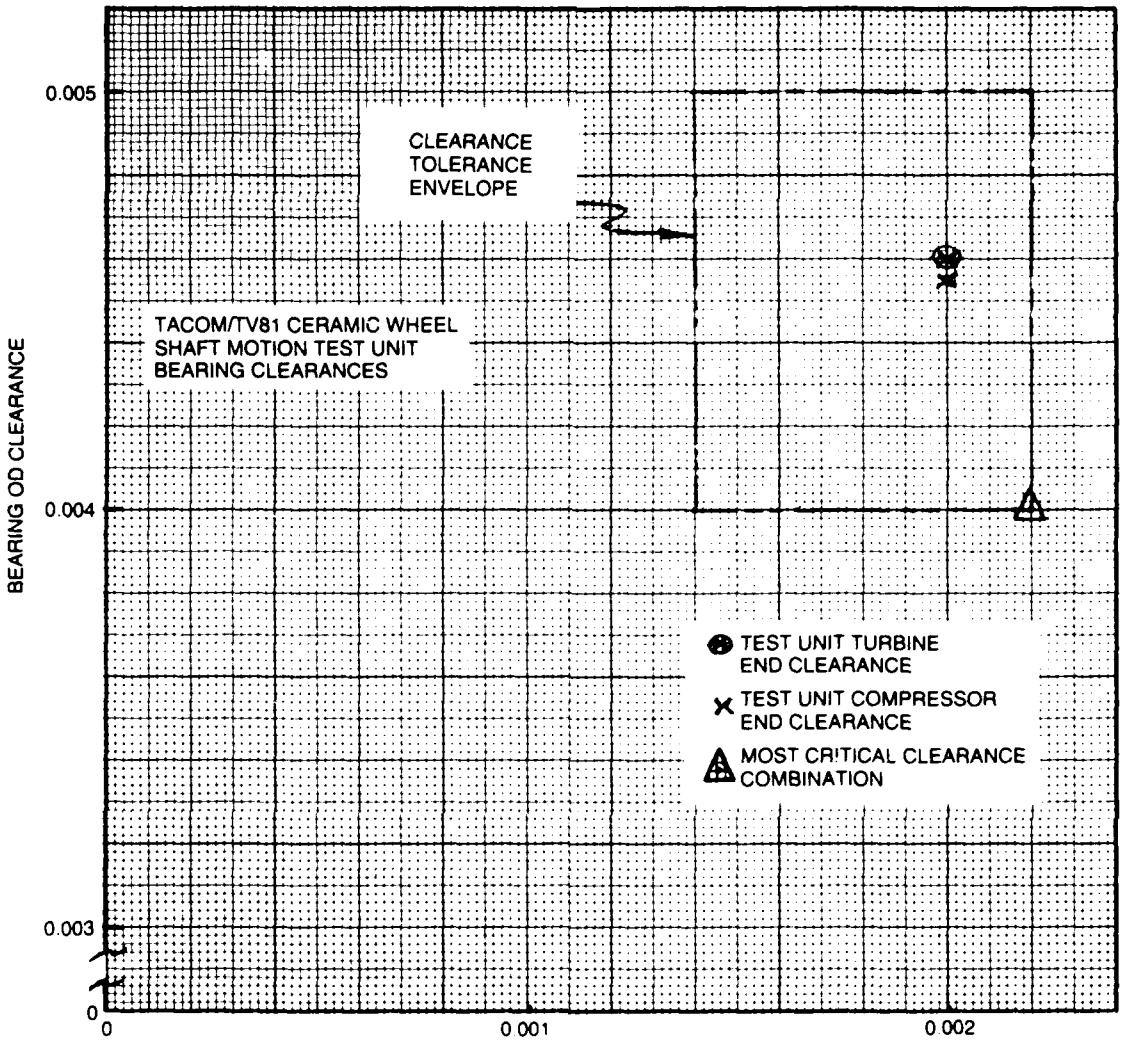

Figure 5-41. TACOM/TV81 Ceramic Wheel Shaft Motion Test Unit Bearing Clearances

components were balanced to standard print tolerances (.0309 gram inch unbalance maximum).

To establish the minimum possible run-out of the special compressor nut on which the proximity probes target, the assembled center housing rotating assembly (CHRA) was put on a surface grinder and with the shaft assembly rotated, by compressed air blown on the turbine blades, the nut was ground true. A photograph of the compressor inlet with the proximity probes and special nut is shown in Figure 5-42.

The maximum radial play was measured at the special compressor nut by skewing the rotating assembly by hand. The oscilloscope traces (before and after the test) are shown in the Appendix D. The maximum total motion was about .023 inches.

In the shaft motion testing, one X-Y plotter is used. As a result, each page of data is taken at a different real time which sometimes leads to differences in results if a comparison is made between a trace and an oscilloscope picture. Figure 5-43 shows a typical shaft motion instrumentation setup.

Garrett has established certain maximum total shaft motion limits which can not be exceeded for an acceptable design. These limits are expressed as a percentage of the maximum possible total motion. The list below shows the limits for this size unit:

Speed Range	Max. Total Motion	Max. 1st Order Motion
Up to 50% Rated Speed	45% (.0104 inch)	20% .0046 inch)*
50% to 110% Rated Speed	30% (.0069 inch)	16% (.0037 inch)

*Only at low speed 1st critical

The rated speed for this application is 71,700 r/min (1195 Hz). For the overspeed tests, 80,000 r/min (1333 Hz) was used which is 112 percent of rated speed.

A sweep from minimum speed (about 10,000 r/min) to 80,000 r/min produced a first-order or synchronous total motion of .0034 (horizontal probe) at 80,000 r/min. This value is close to the maximum allowable of .0037 inch and indicates the unit's unbalance was near the tolerance high limit. No low-speed critical point was observed during this test.

After the sweep test, five steady speed test points were run based on high-amplitude peaks seen on the sweep trace. The conditions under which these points were run are shown in Appendix D.

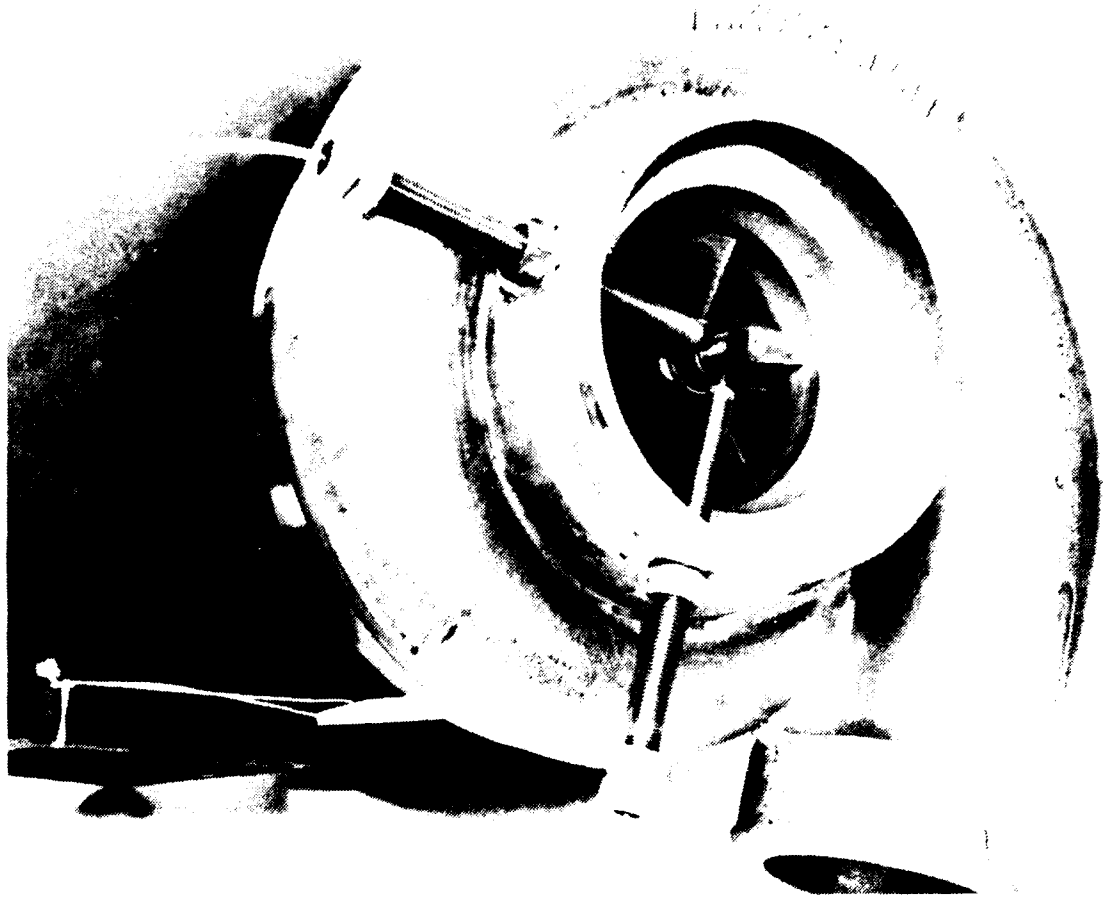

Figure 5-42. Compressor Inlet with Proximity Probes

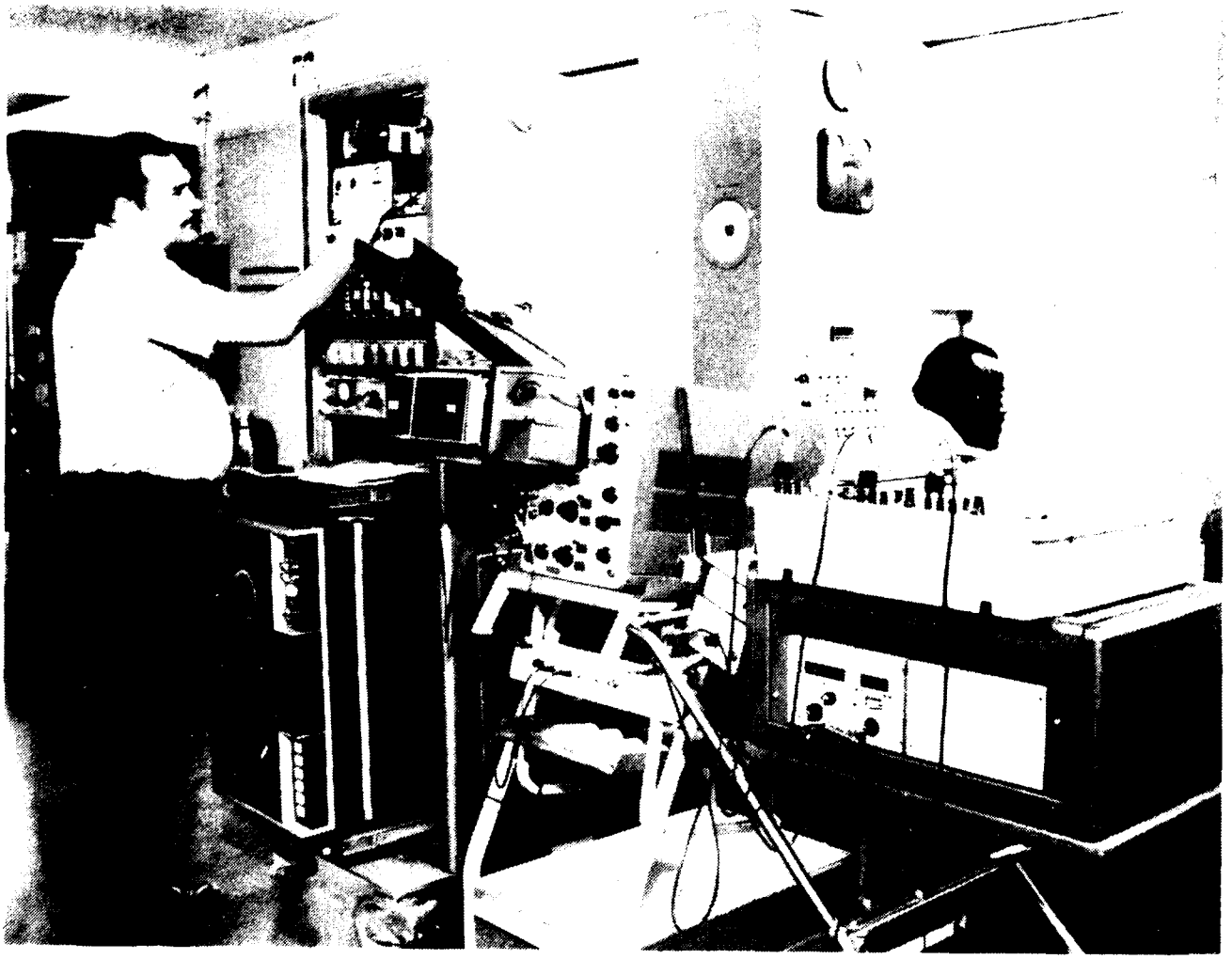

Figure 5-43. Instrumentation Setup for Shaft Motion Test

The maximum full frequency shaft motion occurred at the relatively low speed of 12,000 r/min (or 200 Hz) and was about .0095 (vertical probe) peak to peak. This high value is not seen in the sweep curve, but is shown on the spectral frequency curve and the oscilloscope picture. (See Figure 5-44). The allowable total motion is .0104 inches.

Previous shaft motion tests with metal turbine wheels (see list of References and with different but similar compressor wheels as used with the ceramic wheel tests show very similar full spectrum peak-to-peak amplitudes but at different r/min. Previous results are .009 at 50,000 r/min and .010 at 18,000 r/min. Synchronous amplitudes on previous tests were .0015 at 90,000 r/min and .0010 at 18,000 r/min.

From review of previous metal wheel shaft motion tests and from Garrett acceptable level criteria the TV 81 turbocharger with ceramic turbine wheel has acceptable shaft motion.

5.5.5. Durability Demonstration. The objective of these tests was to obtain laboratory durability information under accelerated duty conditions.

Each turbocharger assembled was installed on a gas stand and gradually accelerated to 80,000 r/min before shipment or further r/min test.

Four complete turbocharger assemblies were durability tested for 100 hours each on an endurance gas stand. These units were cycled from a maximum condition of 80,000 r/min and 649 ^{o}C (1200 ^{o}F) turbine inlet temperature down to the lowest speed obtainable under bootstrap conditions. (Bootstraping is a self-sustained operation with the compressor supplying the flow and pressure necessary to drive the turbine. The turbocharger speed on an 8V92TA rated at 460 Brake Horsepower is 71,700 r/min and, consequently a test speed of 80,000 represents 12 percent overspeed and 24 percent overstress. Each unit was inspected following the test to identify possible problems.

The complete test procedure is explained in Appendix E.

Four ceramic wheel test units (S/N's: TAC 004, 005, 006 and 008) have been successfully run for 100 hours each on cycle endurance. The basic assembled clearances are listed in Appendix E. Unit TAC 008 was first used for shaft motion testing and then was used as the fourth endurance test unit.

A photograph of one of the test units mounted on the bootstrap gas stand is shown in Figure 5-45. (See additional photographs in Appendix E). This same stand was also used for the hot spin tests.

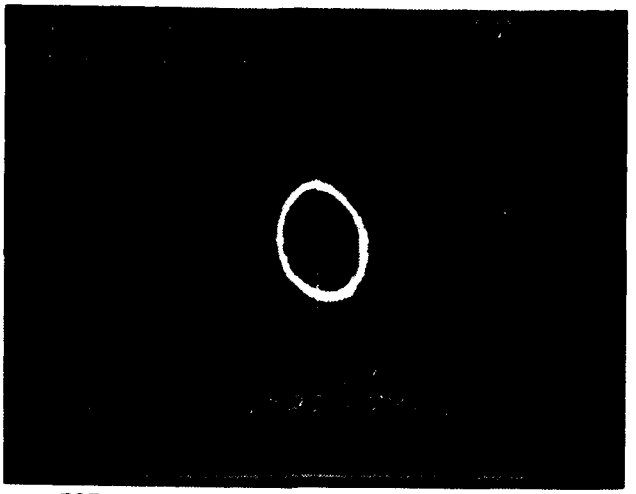

(a) TOTAL MOTION OF 0.0095 INCH AT 200 Hz (12,000 r/MIN)

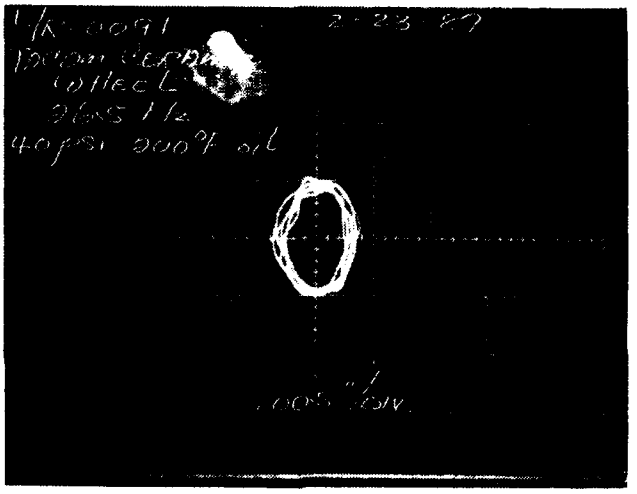

(b) TOTAL MOTION OF 0.009 INCH AT 265 Hz (15,900 r/MIN)

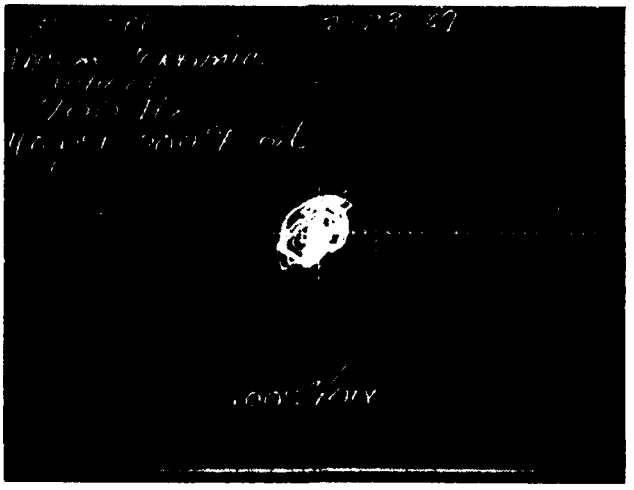

(c) TOTAL MOTION OF 0.007 INCH AT 700 Hz (42,000 r/MIN)

Figure 5-44. Oscilloscope Pictures from Shaft Motion Test

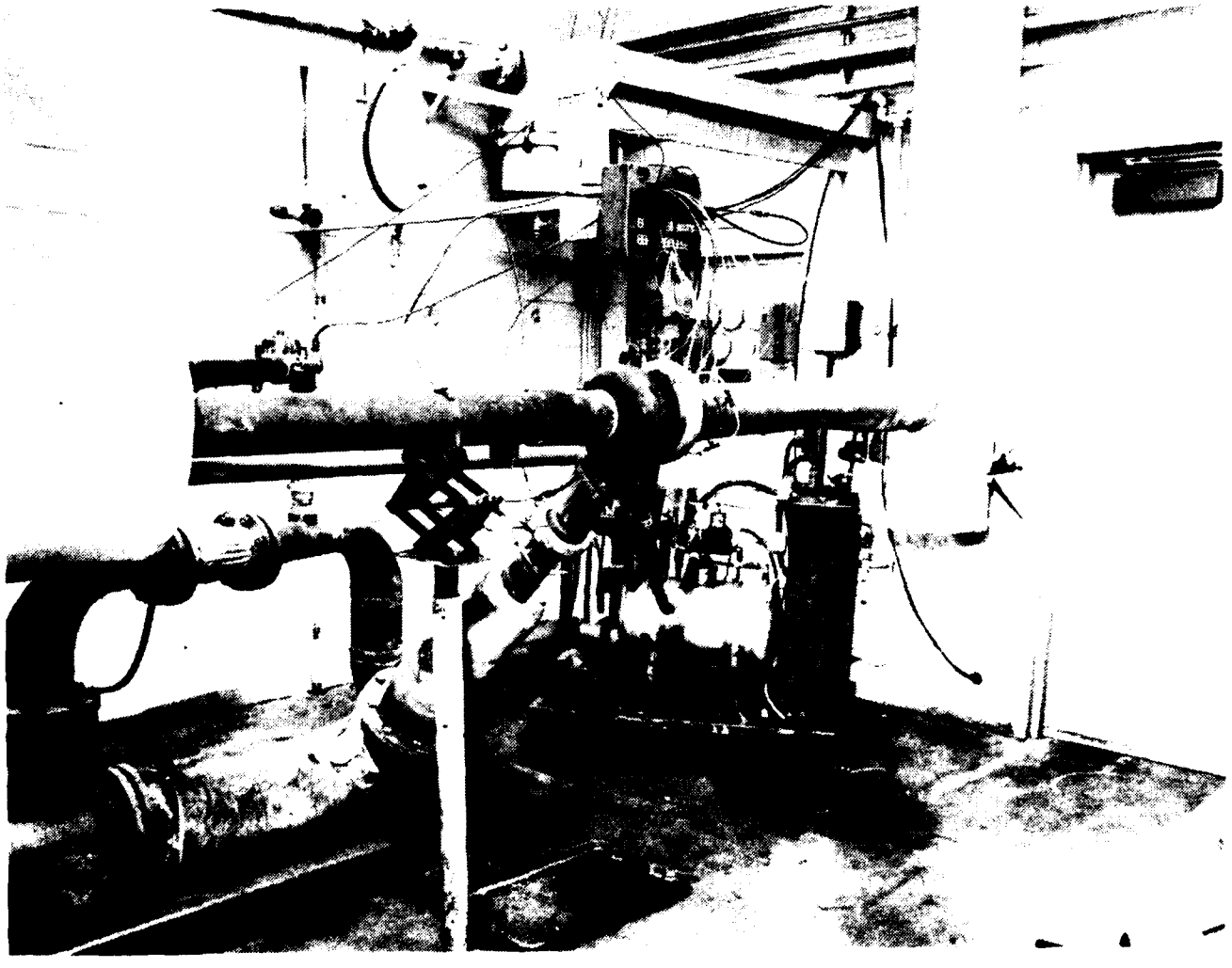

Figure 5-45. Boot Strap Gas Stand Test Setup

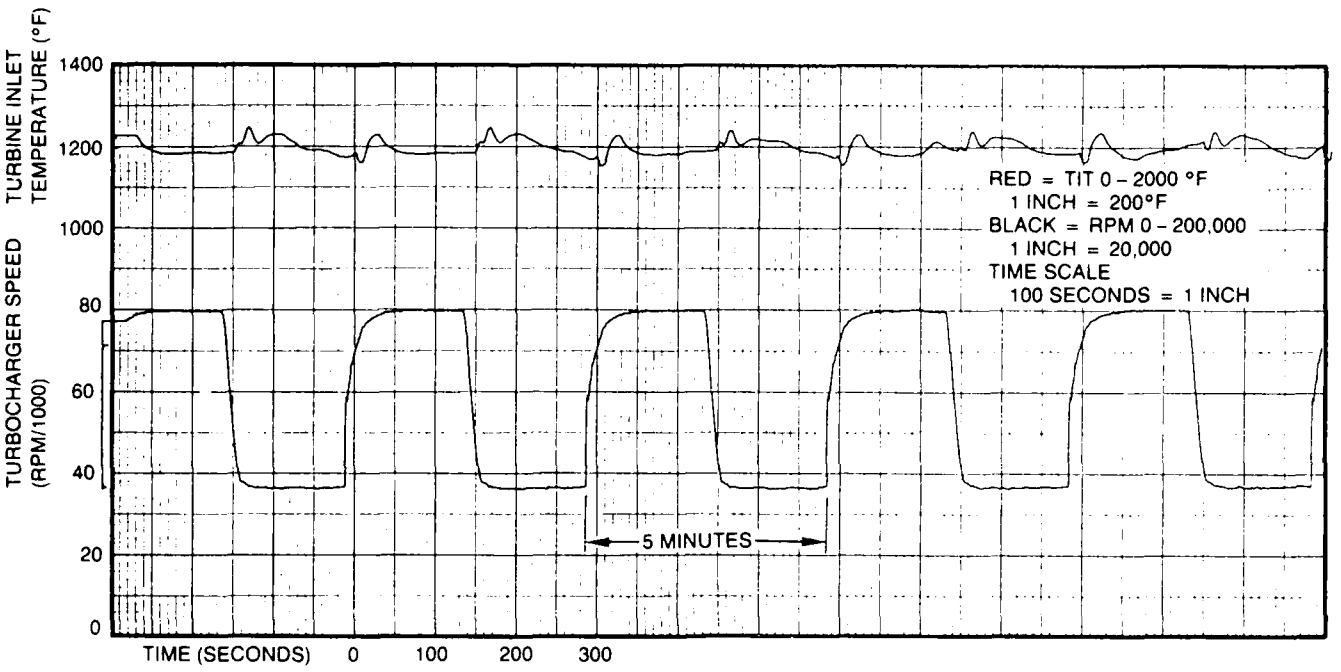

Figure 5-46. Durability Test Cycle

The laboratory test log sheets and a plotted trace of the actual cycle for each of the four units are shown in Appendix E. A typical cycle trace is shown in Figure 5-46.

Inspection of the units after the durability test showed all four to be in excellent condition. The ceramic wheels, which were of main concern, were as new, except for normal light tan combustion deposits.

5.5.6. Static Test. Four point flexural testing was conducted with 40 sample test bars where 20 each were tested at room temperature and 649 C (1200 F) respectively. From this, charactertistic strengths at 63.2 percent failure rate and Weibull modulus' were calculated.

Test bars were machined from the hub sections of TV-81 turbine wheel castings, part number 444310-1. The material was Kyocera International silicon nitride SN-220M. Bar dimensions were .125 by .250 by 2.00 + .005 inches, flat and parallel to + .001 and perpendicularity + 1 degree. All grinding was done in the longitudinal direction to a final surface finish with a 320 grit diamond wheel. No pits or scratches having any dimensions greater than .020 inches were allowed as evidenced by visual, fluorescent dye penetrant (per mil-I-6866 type 1, method B) or radiographic inspection (per ASTM-E-94-68, level 2T-2).

Testing was conducted with a hot-pressed silicon carbide self-aligning fixture (refer to Figure 5-47). Inner and outer spans were .75 and 1.50 inches and the crosshead speed was .020 inches/min. Elevated temperature testing was conducted in air using an electric furnace (refer to Figure 5-48). Specimens were allowed to soak for 15 minutes at test temperatures of 649 C (1200 F) before loading.

The bar size and load span tested at Garrett deviates slightly from Mil Standard 1942. This is due to the large data base of testing established over the last 10 years.

Ambient temperature testing of 20 specimens produced a characteristic strength of 115.1 Kips Per Square Inch (KPSI) and Weibull modulus of 13.5. At 649 C (1200 F), the group characteristic strength was 101.2 KPSI and modulus of 10.9. A tabulation of the test data points are presented in Appendix F. Kyocera published four point flexural strengths versus temperature are shown in Figure 5-49 with the two Garrett test points. Extrapolating the Garrett points upward with temperature tends to point to the knee in the Kyocera curve where in this temperature range, strengths normally decline. Figures 5-50 and 5-51 are corresponding two parameter Weibull plots depicting slope and failure distribution. The values obtained from this test are sufficient to exceed the predicted requirements to provide .1 percent failure at rated speed.

Figure 5-47. Hot/pressed Silicon Carbide Self-Aligning Fixture

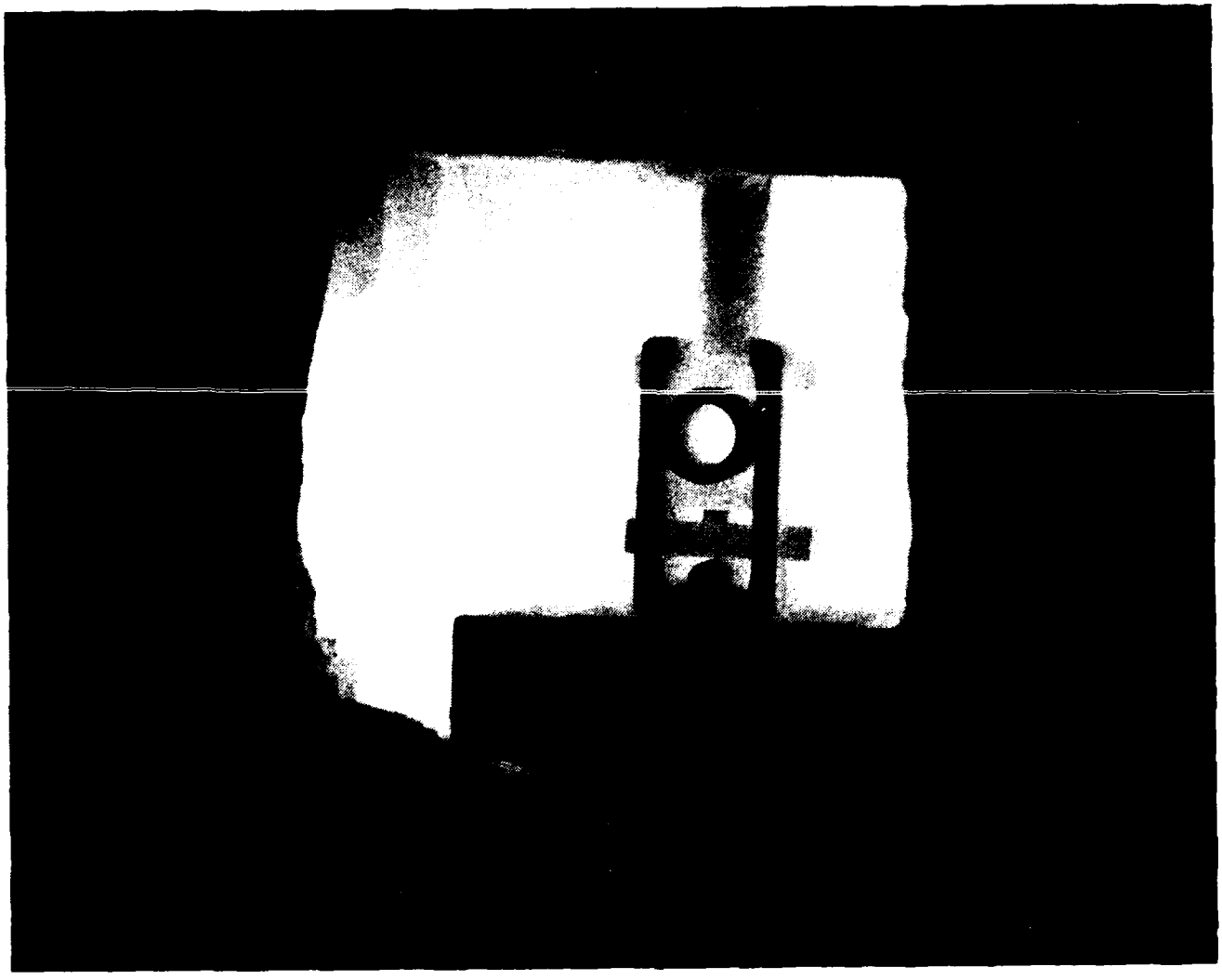

Figure 5-48. Electric Furnace for Elevated Temperature Test

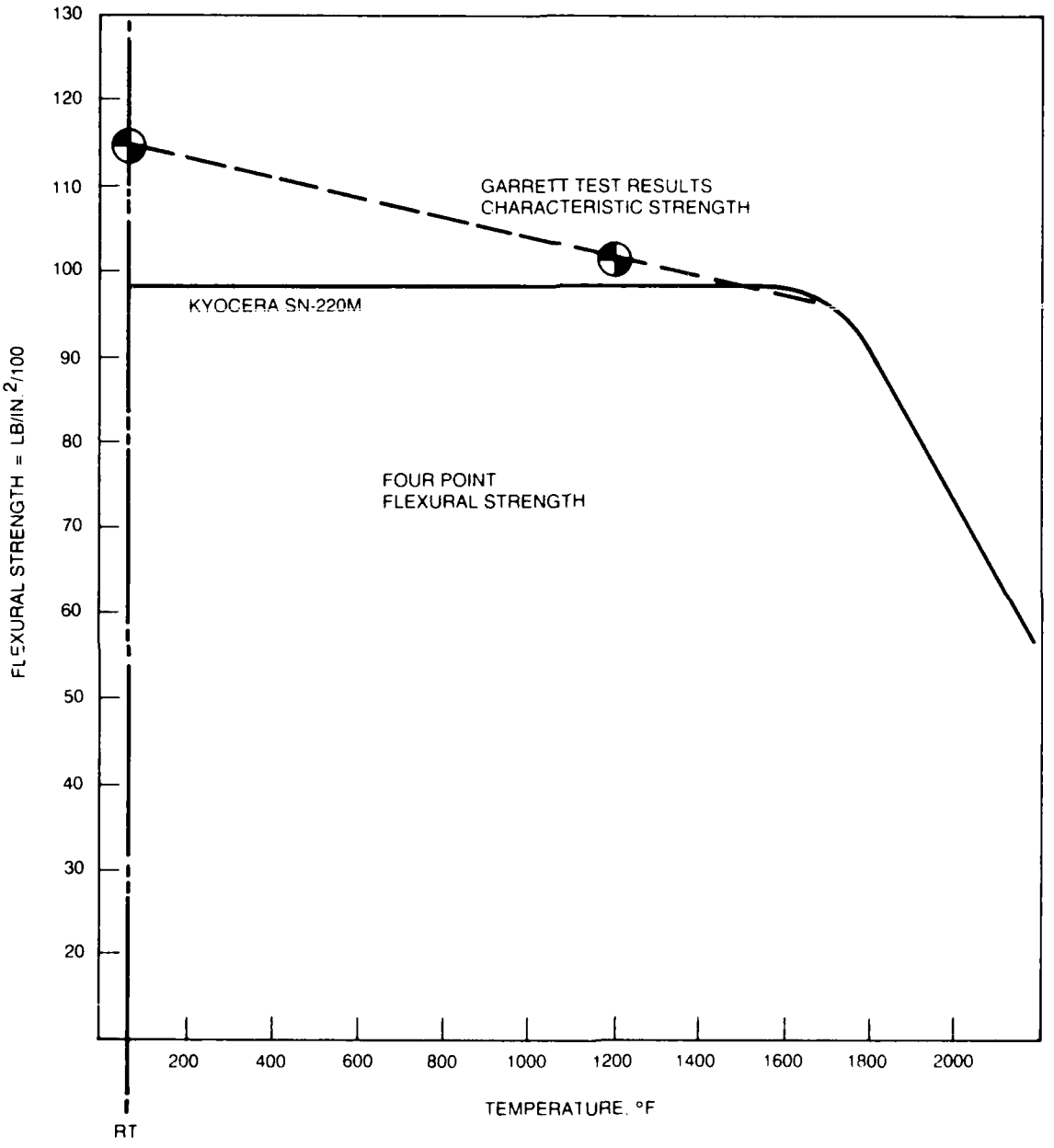

Figure 5-49. Four Point Flexural Strength

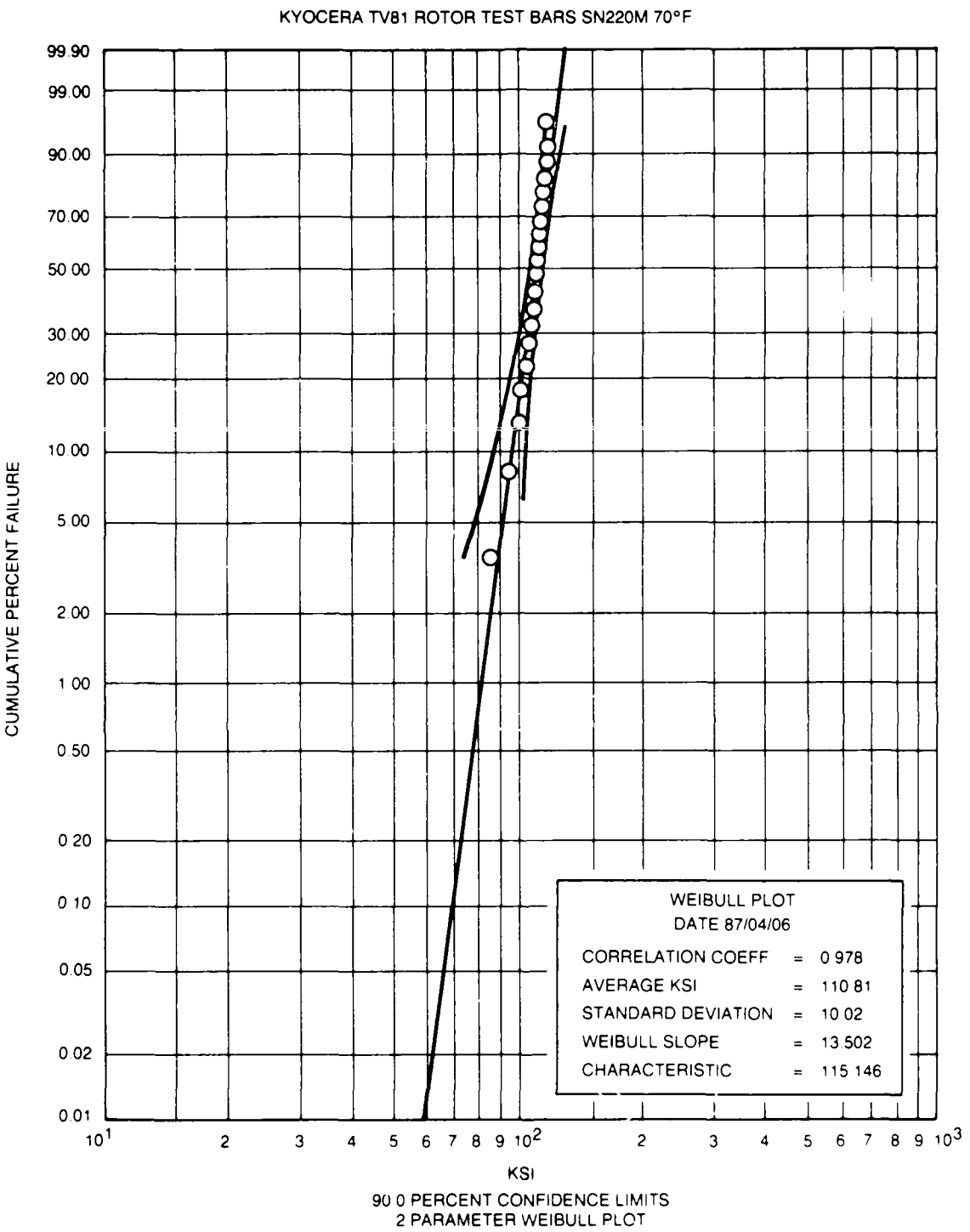

Figure 5-50. Four Point Bending Test Weibull Distribution ... Ambient Temperature (20 Specimen).

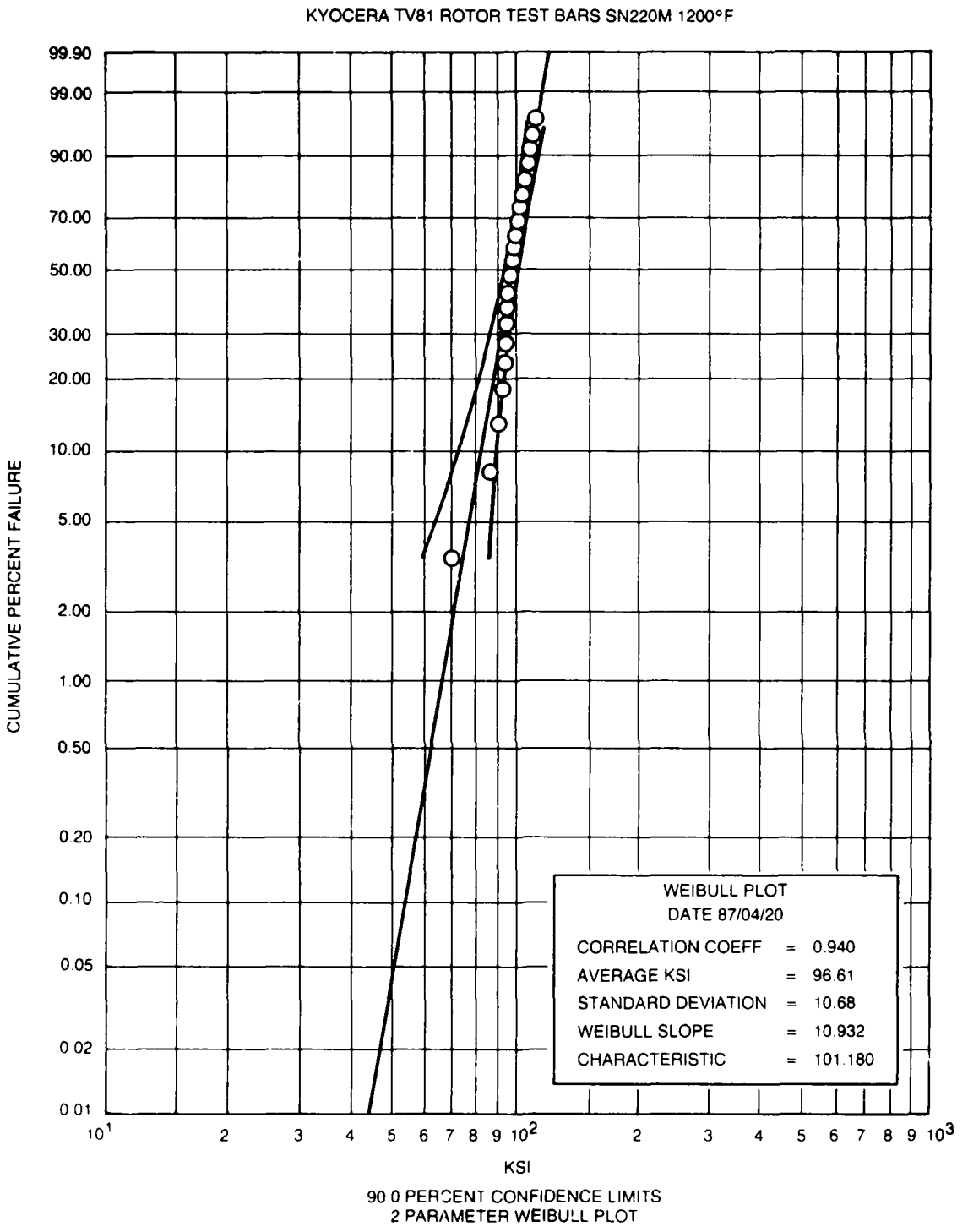

... -1. Four Point Bending Test Weibull Distribution
... Elevated Temperature (20 Specimen)

In each of the 2 groups of 20 specimens, one point seemed to fall low. The effect of these points on characteristic strength and Weibull modulus are shown on Figures 5-52 and 5-53. Ambient temperature characteristic strength was 115.9 KPSI and Weibull modulus of 21.3. At 649 ^{o}C (1200 ^{o}F), the characteristic strength was 101.3 KPSI and modulus of 15.9. Thus, neglecting the 1 low point in 20 has a lesser effect on strength, but a dramatic increase of Weibull modulus.

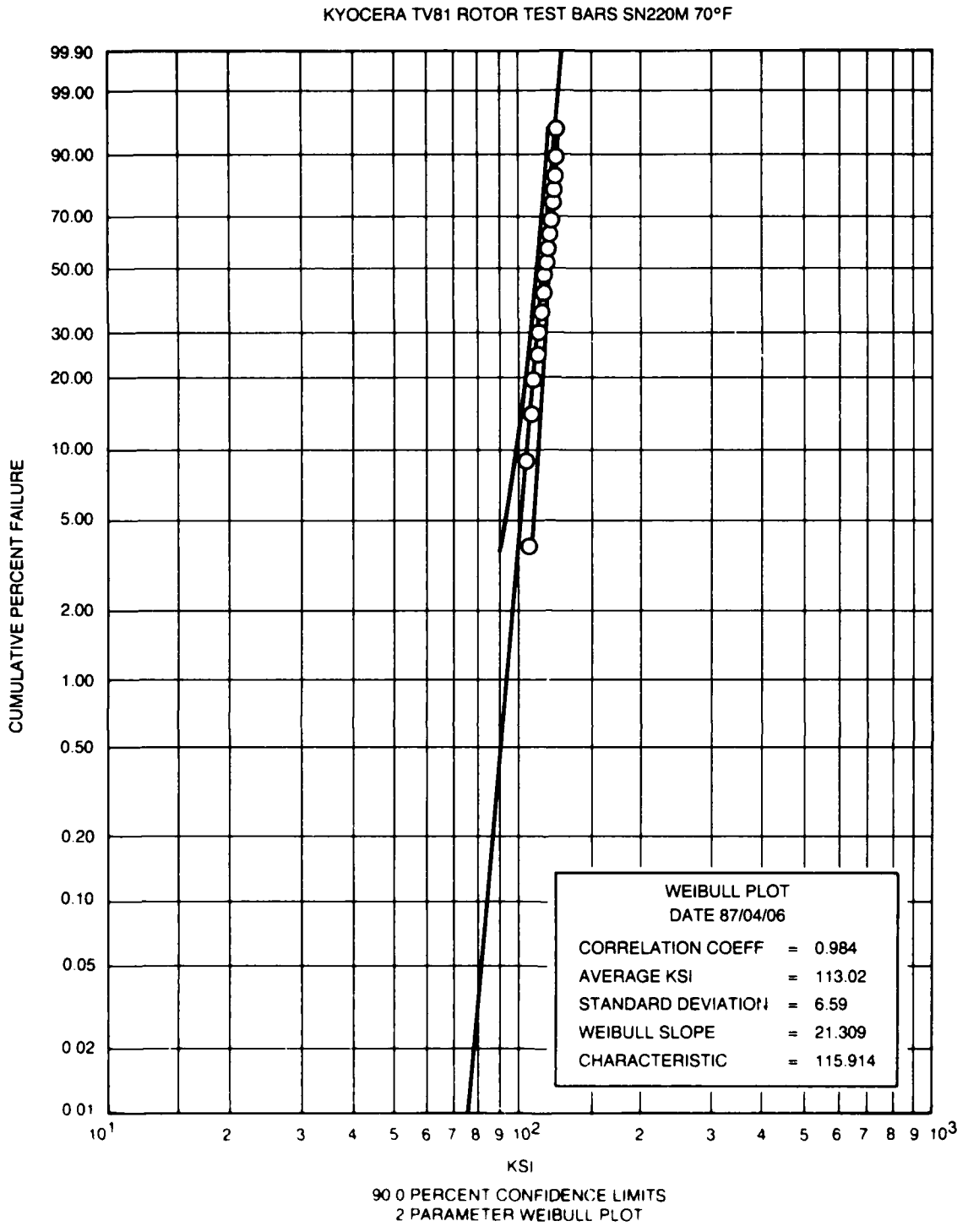

Figure 5-52. Four Point Bending Test Weibull Distribution ... Ambient Temperature (10 Specimen)

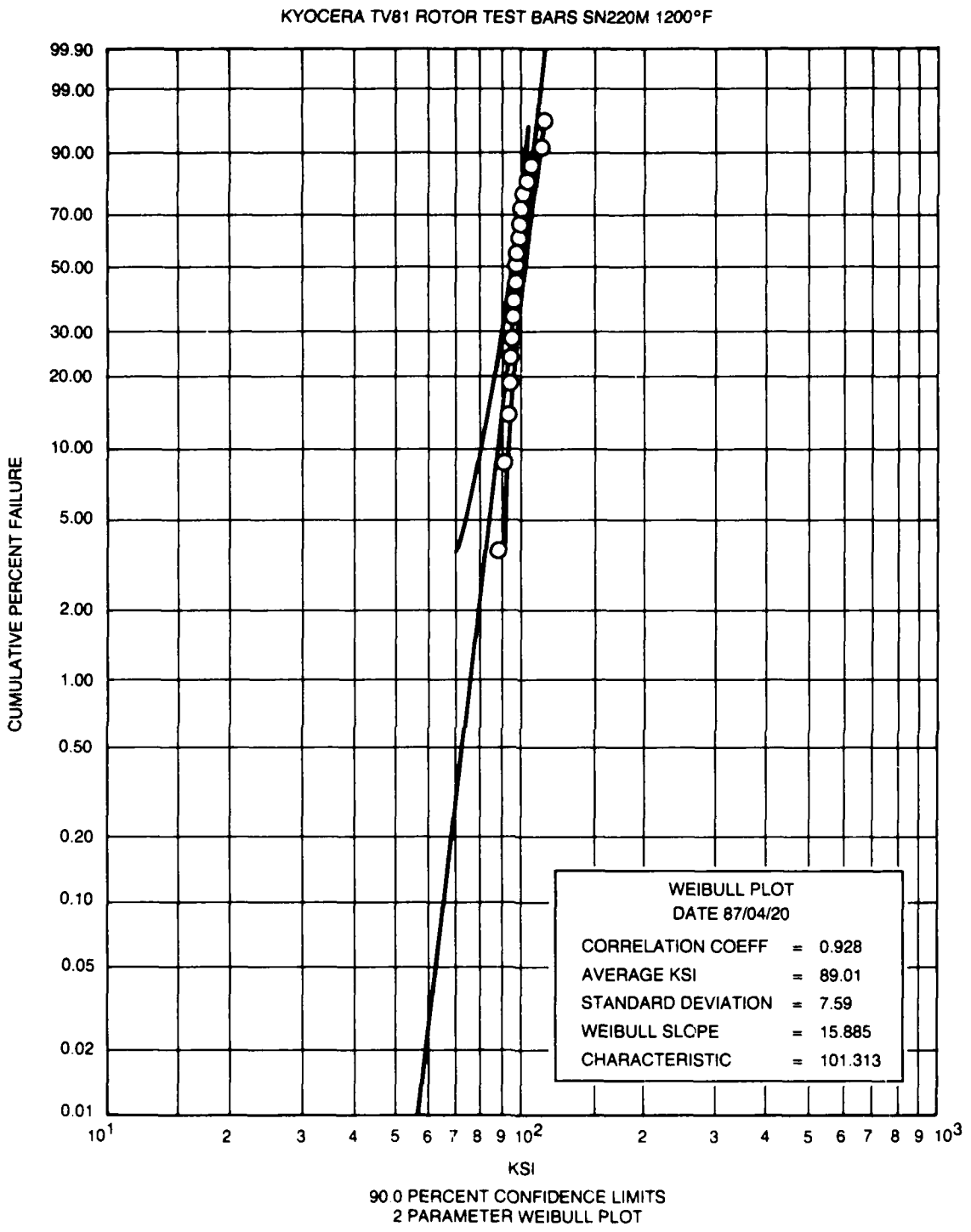

Figure 5-53. Four Point Bending Test Weibull Distribution ... Elevated Temperature (19 Specimen)

LIST OF REFERENCES

1. Hamano, Y., Sagawa, N., Miyata, H., "Reliability Evaluation of Ceramic Rotors for Passenger Car Turbochargers", Journal for Engineering for Gas Turbine and Power, The American Society of Mechanical Engineers, New York, N.Y., Volume 108, Page 531 to 535 (July, 1986).

2. Eclestrom, R., "TV81 Shaft Motion with Extended Backdisc Impeller", Report No. 20.670R, Garrett Automotive Group, Allied Signal Corporation, Torrance, CA (April, 1975).

3. Zimmerman, E., "TV81 Shaft Motion Test for Qualification of Backcurved Impeller", Report No. 8TR28-001, Garrett Automotive Group, Allied Signal Corporation, Torrance, CA (February, 1978).

SELECTED BIBLIOGRAPHY

Eclestrom, R., "TV81 Shaft Motion with Extended Backdisc Impeller", Report No. 20.670R, Garrett Automotive Group, Allied Signal Corporation, Torrance, CA (April, 1975).

Hamano, Y., Sagawa, N., Miyata, H., "Reliable Evaluation of Ceramic Rotors for Passenger Car Turbochargers", Journal for Engineering for Gas Turbine and Power, The American Society of Mechanical Engineers, New York, N.Y. Volume 108, Page 531 to 535 (July, 1986).

Zimmerman, E., "TV81 Shaft Motion Test for Qualification of Backcurved Impeller", Report No. 8TR28-001, Garrett Automotive Group, Allied Signal Corporation, Torrance, CA (February, 1978).

END

DATE

FILMED

5-88

DTIC